Revised Manuscript (clean copy)

Click here to view linked References

New insights on the origin of Barra Volcanic Ridge System, offshore Ireland: a long-distance influence of the Iceland mantle plume

Gaurav Tomar[1,2,5], Srikumar Roy[2], Christopher J. Bean[1,2], Satish C. Singh[3], Brian O'Reilly[1,2] and Nick Schofield[4]

1. Geophysics Section, Dublin Institute for Advanced Studies, 5 Merrion Square, Dublin 2, Ireland

2. Irish Centre for Research in Applied Geosciences, University College Dublin, Dublin 4, Ireland

3. Marine Geosciences, Institut de Physique du Globe de Paris, 1 rue Jussieu, France

4. Department of Geology and Geophysics, University of Aberdeen

5. Now at CSIR, National Institute of Oceanography, Goa, India

Abstract

The Iceland Plume has significantly impacted the North Atlantic region. Igneous edifices and large seamounts in the Rockall region were linked to Iceland plume pulsations during the Late Cretaceous to Mid-Eocene. In the south of the Rockall Basin a chain of northwest-southeast trending volcanic ridges known as the Barra Volcanic Ridge System (BVRS) have been identified on seismic and magnetic datasets. However, the timing, morphology, extent, and emplacement mechanism of the BVRS are not well understood. To investigate the volcanic ridge system, we analyze a 360-km-long pre-stack time migrated seismic section along the margin, which covers the southern extent of BVRS. The high velocity (4.5-4.8 km/s) obtained by using first arrival travel time tomography of downward continued data set, high magnetic anomaly and the typical morphology of the ridges suggest that they could be volcanoes of basaltic compositions. The integration of gravity and seismic data constrain the crustal structure and thickness, which indicates that the crust could be as thin as 4 km beneath the BVRS, requiring a maximum stretching factor > 6. Folded compressional structures and lava flows within the Early Paleocene to Mid-Eocene sediments draping the volcanic ridges, suggest that these volcanic intrusions possibly have occurred post Early Paleocene age, which is approximately the same time-period when Iceland mantle plume arrived in the Rockall region.

These results suggest that the BVRS developed because of pre-existing lithospheric configuration in the Rockall Basin and could be one of the southernmost volcanic provinces of the North Atlantic Igneous Province (NAIP).

1. Introduction

The dynamics and topographic expression of continental rifting are impacted by plume-lithosphere interactions (Burov and Gerya, 2014; Koptev et al. 2016); as plume emplacement impacts a larger area beyond its initial point of inception, for example, the African Superplume (Ebinger and Sleep, 1998). The North Atlantic Igneous Province (NAIP) is one of the best-studied volcanic rifted continental margins (White and McKenzie, 1989; Saunders et al. 1997; Hopper et al. 2003; Parnell-Turner et al. 2014; Gaina et al. 2017; Horni et al. 2017; Martos et al. 2018; Steinberger et al. 2019), and an ideal region to study plume-lithosphere interaction in the Northern Atlantic (Howell et al. 2014).

Plume-induced volcanism has been observed in the North Atlantic from east to west Greenland (Horni et al. 2017; Gaina et al. 2017; Steinberger et al. 2019). On the Norwegian-UK side of Atlantic it stretches towards the western margin of the Rockall Plateau, more than 1,000 km southwest of the plume centre (White and McKenzie 1989; Saunders et al. 1997; Steinberger et al. 2019). The Early Paleogene NAIP basaltic rocks extend roughly in NE–SW direction for more than 1000-2500 kms along the East Greenland – NW European margins and are spread out over a vast geographic region: West Greenland–Baffin Island, SE Greenland, NE Greenland, Faroe Islands, Faroe–Shetland Basin (FSB), Britain, Ireland, the Rockall–Hatton area, and the Rockall Basin (Saunders et al. 1997).

Stoker et al. (2017) identified four main rifting periods along the NE Atlantic margin: (1) Devonian–Carboniferous; (2) Permian–Triassic; (3) Jurassic–Early Cretaceous; and (4) Late Cretaceous–Paleocene. The Late Jurassic–Cretaceous intra-continental rifting caused approximately 50–70 km of crustal extension and subsequent Cretaceous basin subsidence from the Rockall Basin-North Sea area to the SW Barents Sea. In early Late Cretaceous times, a renewed rifting occurred in the Rockall Basin and Labrador Sea associated with the northward propagation of North Atlantic seafloor spreading. The Rockall rift apparently became inactive when sea-floor spreading was approached in the Labrador Sea. The final NE Atlantic rift episode caused c. 140 km extension, which began near the Campanian-Maastrichtian boundary, and lasted until continental separation near the Paleocene-Eocene transition. Skogseid et al. (2000) suggested that the late syn-rift and the earliest seafloor spreading periods were affected by widespread igneous activity across a c. 300 km wide zone along the rifted plate boundary. The Rockall Basin is one of the heavily intruded parts of the NAIP volcanic sill province similar to the FSB and Norwegian Margin (Magee et al., 2014).

The Rockall Basin is a failed rift and considered to be a magma poor basin, where no significant volcanic activities are observed (O'Reilly et al. 1996; Pérez-Gussinyé et al. 2001). Overall low magnetic anomaly intensities are observed within the basin (Kimbell et al. 2010) owing to the absence of significant volcanism. In magma-poor continental margins, the crust becomes highly stretched and leading to the thermal cooling, which results in crustal embrittlement (Pérez-Gussinyé and Reston, 2001) allowing faults to crosscut the entire crust facilitating ocean-water circulation to the mantle and resulting in mantle serpentinisation (O'Reilly et al. 1996).

The Irish Rockall Basin is largely under-explored, unlike the UK Rockall Basin (Broadley et al. 2020; Schofield et al. 2018). In the south of the Rockall Basin a series of northwest-southeast trending volcanic ridges known as the Barra Volcanic Ridge System (BVRS) were identified by Scrutton and Bentley, (1988). They suggested that these ridges are extrusive bodies and developed during the Early Cretaceous period. The sedimentary thickness and the nature of the underlying crust of the Rockall Basin has been a matter of debate (Smythe, 1989). It was also suggested that the crust could be oceanic in nature beneath the Rockall Basin (e. g.; Roberts, 1975, Kristoffersen, 1978; Russell and Smythe, 1978; Bentley, 1986 Smythe, 1989). The consensus of more recent studies is that a highly stretched thin continental crust exists beneath the Rockall Basin (e.g., Shannon et al. 1994, 1999; Hauser et al. 1995; O'Reilly et al. 1996; Mackenzie et al. 2002; Morewood et al. 2005; Archer et al. 2005; Naylor and Shannon, 2005).

Wide-angle refraction data imaged beneath the igneous sills and resolved the crustal to upper mantle structure of the Rockall Basin. The wide-angle seismic data indicates an upper mantle velocity of 7.5-7.7 km/s in the Rockall Basin (Morewood et al. 2005). The P-wave velocities and Vp/Vs ratios of the sub-crustal mantle layer beneath the Rockall Basin is more consistent with upper mantle serpentinisation rather than magmatic underplating (O'Reilly et al. 1996; Morewood et al. 2005). Mantle serpentinisation has also been suggested in the adjacent Porcupine Basin, based on multi-channel and wide-angle seismic data (Reston et al. 2001; Prada et al. 2017; Tomar et al. 2022) and 3D seismic data set (Lymer et al. 2022).

In the Rockall Basin the age, morphology, extent, and emplacement mechanism of the BVRS has not been investigated using recently acquired geophysical data. In an attempt to investigate the BVRS in the southern Rockall Basin, a model of the BVRS is presented here that defines the approximate timing of its formation and its spatial-temporal setting in a North Atlantic context in the absence of any nearby well data or dating of basalts. We illustrate the interpretation of volcanic ridges associated with the BVRS on a high-resolution seismic profile (for location see Figure 1, 2) and provide an estimation of the bulk crustal stretching factor (β) distribution in the south of the Rockall Basin. We further illustrate crustal to upper mantle structure along the margin of the Rockall Basin and the relationship of the BVRS with the NAIP.

2. Geological Setting

The Paleocene-Eocene continental breakup in the North Atlantic is linked to the origin of the NAIP (Doré et al. 1999). Two phases of volcanism related to the NAIP have been observed: a) at the late Paleocene- early Eocene (~62-58 Ma) and b) ~57-52 Ma (Wilkinson et al. 2017; Peace et al. 2018, 2020). For example, the volcanism is observed during Eocene period (~56-57 Ma) in western Greenland (Pedersen et al. 2002), Baffin Island (Stuart et al. 2003), eastern Greenland, Britain and Ireland (Figure 1) (Torsvik et al. 2001). The basaltic lava erupted from beneath thick continental lithosphere, at ~ 61 Ma, simultaneously, from Baffin Island to the western and eastern margins of Greenland, and at ~57 Ma from the Faeroe Islands (Jolley et al. 2021), to western Britain and NE Ireland, a roughly circular area with diameter 2000 km (Storey et al. 2007; Horni et al. 2017).

Figure 1 illustrates the main volcanic facies in the Faroe-Rockall-Hatton area, which is dominated by basaltic volcanic rocks derived from many different sources and includes numerous volcanic centres. Pre-breakup to breakup volcanism is represented by the landward lava flows and inner flows (Figure 5 of (Horni et al., 2017)), which cover much of the Faroese, UK and Irish margins over a broad area (Horni et al. 2017; Celli et al. 2021). Sampling and dating of volcanic rocks from the landward and inner flows along the Rockall–Hatton margins shows that these units include both pre-breakup and breakup volcanic rocks and that the pre-breakup phase is less extensive. Landward flows are locally important; with the Rockall-Hatton region having significant coverage (Figure 4 of Horni et al., 2017). It is also observed by Horni et al. (2017) that there exists significant volcanic asymmetry between SE Greenland and the Hatton-Rockall margin.

Britain, Ireland and the adjacent continental margins have experienced several episodes of Cenozoic exhumation during Paleocene, Eocene–Oligocene and Miocene (Holford et al. 2009; Stoker et al. 2010). The regional episodes of exhumation in Britain, Ireland and the neighboring Rockall and Porcupine basins (west of Ireland) that occurs at the Paleocene-Eocene boundary correlates with the early Paleogene uplift that is interpreted to have formed due to the initial emplacement of the NAIP (Jones et al. 2002; Holford et al. 2009; Stoker et al. 2010).

The Rockall Basin mainly consists of the continental lithosphere and is one of the largest Irish deep sedimentary basins, located along the North Atlantic continental margin (Figure 1) (Roberts et al. 1988; England and Hobbs, 1997; Morewood et al. 2005).

The rifting age of the Rockall Basin is still in dispute. Most of the studies suggested the main phase of extension which led to the hyper-extension of the basin occurred during the late Jurassic to early Cretaceous period (England and Hobbs, 1997; Cole and Peachey, 1999; Shannon et al. 1999; Roberts et al. 2019). Schofield et al. (2018) proposed a Triassic rifting as well as Late Jurassic-Early Cretaceous rift phase. Rifting in the Rockall Basin created a thin continental crust, several wide-angle seismic and gravity studies suggest a stretching factor in the range of ~4-6 (Joppen and White, 1990; Shannon et al. 1999; Readman et al. 2005; Morewood et al. 2005; Welford et al. 2010; Kimbell et al. 2010; Shannon, 2018).

Known igneous centres including the saucer-shaped igneous sill complexes and basalt lava flows of Late Cretaceous to Mid Eocene, in north of the Rockall Basin have been suggested to be part of the NAIP (e.g., Archer et al. 2005; Magee et al. 2014; Wilkinson et al. 2017; Horni et al. 2017). The BVRS was proposed as early Cretaceous extrusive events based on old seismic data set and correlation with the volcanic activities in surrounding area like the Porcupine Basin (Scrutton and Bentley, 1988; Kimbell et al., 2010). Gernigon et al. (2004) suggested that sill intrusions and vents near the BVRS were of Paleogene in age. Poor-quality of seismic data and lack of dating on borehole data have previously hindered the determination of the actual age of the BVRS. Dating of the igneous edifices and seamounts in the Rockall-Hatton region linked them to episodic Iceland plume pulsations (O'Connor et al. 2000). Stoker et al. (2017) suggested that because of the pre-existing lithospheric configuration the volcanic material could be channeled into the Rockall–Hatton margins. Due to the close proximity of the Rockall-Hatton region to the Iceland mantle plume this region could be preferred region for lateral flow of plume material (Horni et al. (2017).

3. Data: Seismic, magnetic and gravity

An integrated approach using seismic, gravity and magnetic data is used to investigate the nature of the BVRS as well as its settings within the crustal to upper mantle structure of the Irish southern Rockall Basin. The bathymetric data used in Figure 1 has been adopted from the General Bathymetric Chart of the Oceans (GEBCO, Monahan, 2008) and includes high-resolution INFOMAR data obtained from the Irish National Seabed Survey conducted jointly by the Marine Institute of Ireland and Geological Survey of Ireland (Figure 2a). The location of seismic profile (PAD14-028) used in this study crosses the NW-SE trending BVRS (Figure 1, 2a, 3b) as well as the highest gravity anomaly (Figure 3a) in the Rockall Basin.

The study area comprises of the deep water setting of the Rockall Basin that lacks deep-stratigraphic borehole data, specially the central and southwestern region. The only wells drilled in the central part of Rockall are shallow boreholes, which do not penetrate older than Oligocene sequences. The ODP Leg 162 Site 981A borehole, located in the north-western part of the Rockall Basin, provides some control on the younger Cenozoic (Pliocene-Pleistocene) sequences. Three wells were drilled on the northeastern flank of Rockall Basin, 5/22-1 (which proved a thick Cenozoic succession, overlying the uppermost Cretaceous – Top Shetland Group), and two wells in the 12/2 block, relating to the Dooish discovery, which encountered sandstone reservoirs of Permian to Middle Jurassic age containing rich gas condensate.

The high-resolution PAD-13 and PAD-14 seismic profiles were acquired by R/V BGP Explorer for ENI Ireland BV during 2013–14. The vessel was equipped with Sercel G-Gun-II as a source, placed at a depth of 8 m (+1 m), and towed a 10,050 m long streamer at 10 m (±1 m) depth. The shot-point interval was 37.5 m, the record length 12s sampled at 2 ms. The Pre-stack Time Migration (PSTM) was performed by implementing standard industry signal processing steps and performing seismic velocity analysis. As, the seismic profiles are spaced at 40–50 km, the correlation of the volcanic ridges is difficult, and therefore, we integrate the gravity modeling results to better constrain the crust and upper mantle structures. Due to lack of deep well data in the study area, we correlated our seismic horizon interpretation with the seismic composite line interpretation done by Merlin Energy Resources Consortium (MERC ,2020).

The gravity data (Figure 3a) from Sandwell et al. (2014), is used in this study to investigate the large-scale crustal structure. It has a resolution of 2 mGal. A comparison between satellite (Sandwell and Smith, 1997) and ship-borne gravity measurements across the Irish continental shelf was carried out and observed an agreement within ~4 mGals (Readman et al., 2003). The new gravity data was acquired during the acquisition of the DCENR–ENI seismic data in the Porcupine and Rockall Basin (Geotrace Technologies Ltd., 2015). Tomar and O'Reilly, (2020) compiled this data with the satellite gravity data (Sandwell et al. 2014) and observed a good agreement (within ~2 mGals). Therefore, the satellite gravity data (Sandwell et al. 2014) was used for gravity modelling. The magnetic data (Figure 3b) is used from Verhoef et al. (1996). The final grid for the magnetic data was merged from 886 different shipboard missions between 1956-1992, which has a 5 km cell size and a 50 W meridian. The cell size in the data set eliminates the anomalies that has shorter wavelength than 10 km. However, the major magnetic anomalies in the study region are resolved. The PAD magnetic data was also acquired during DCENR–ENI seismic data acquisition. We compare PAD magnetic data with Verhoef et al. (1996) magnetic data (see section 5) and found major difference between these data sets. Hence, PAD data is used for magnetic modelling in this study. The 2D sub-surface structures and magmatic bodies in the Rockall Basin were identified using gravity and magnetic data sets (O'Reilly et al. 1996; Readman et al. 2005; Kimbell et al. 2010), which we have used as a base model for this study.

4. Downward continuation and Travel time tomography

The PAD14-028 seismic line crosses three magnetic highs (VR2, VR3 and VR4 in Figure 3b) which were collectively interpreted as the BVRS (Scrutton and Bentley, 1988) using the seismic data then available. The seismic line crosses a fourth magnetic high (VR1) which is recognized at the edge of the Charlie Gibbs Fracture Zone (CGFZ) and considered to be a part of the Charlie Gibbs Volcanic Province (Keen et al. 2014). The seismic section is shown in Figure (4a) and the seismic interpretation is shown in (b). Before, performing travel time tomography (TTT), downward continuation (DC; Arnulf et al., 2011) was carried out for enhancing the first arrival which turn in the upper crust. Bandpass filtering and frequency time filtering was implemented prior to applying downward continuation.

A downward extrapolation was performed to a depth of 200 m above seafloor to create a synthetic On-Bottom experiment. A Kirchhoff integration scheme and a water velocity of 1485 m/s were used for downward extrapolation (Berryhill, 1984). A slowness range of 0.68 - .18 s/km were used for DC. Here, we applied a first pass of the DC, i.e., we place all the receivers at a datum above the seafloor. The datum was kept at 200 m above the seafloor to avoid the surface waves, because if we keep the datum too close to the seafloor it creates an impression of the surface wave in synthetic data (Audhkhasi and Singh, 2019).

The DC enhances the first arrivals due to better ray coverage in the upper crust, and it provides better resolution for the upper sedimentary sequence velocities. Thus, the downward extrapolated gathers have larger offset ranges for the first arrival from 3.5 km to 9.4 km (Figure S1b) in comparison to the raw shot gather from 5.5 km to 9.8 km (Figure S1a). The DC of streamer data normally has two steps, first we put our receivers at a particular datum and secondly, we place all the sources at the same datum. We would lose the data (same as the streamer length, 10 km) in the beginning and end of the seismic profile while sorting the shot gathers to receiver gathers for second step of the DC. It would have affected obtaining the velocity of VR1. The smiling effect of DC at far offset limits the first arrival picking, which could hinder the velocity of the deeper volcanic structure (VR4). Therefore, only first step of the DC is performed in this study. The first arrivals were picked from DC data to perform TTT (Van Avendonk et al., 2004).

A ray-based TTT of the enhanced first arrivals on the DC shot gathers was performed to obtain a smooth P-wave velocity model of the upper crust (Van Avendonk et al., 2004) and the ray tracing is performed using shortest path method (Moser et al. 1992). The first arrival of every fifth shot at 187.5 m spacing was picked to reduce the picking time for TTT without compromising the lateral resolution. In total 1920 from 9600 shots travel time were picked along the profile. A semi-automatic picking strategy were adopted to optimize the time and to facilitate the shot-to-shot continuity. The final picking uncertainty is set to 15 ms depending on the seafloor depth, shot-receiver position uncertainty, and downward extrapolation uncertainty (Ghosal et al. 2014; Huot et al., 2018). A 1-D model was used to create a 2-D starting velocity model (Figure 5a) for first iteration of inversion which was converged to minimum misfit (χ^2) ensuring adequate smoothing. The 1-D model was built based upon the velocity models of O'Reilly et al., (1996) and Mackenzie et al., (2002) for the upper crustal structure. A higher regularization was applied in the horizontal direction as compared to vertical direction (1/4th of the horizontal) in all iterations to obtain a laterally smooth model.

Many inversion iterations were performed with the starting model until χ^2 converged close to unity. In vertical and horizontal directions, the graph grid spacing for ray tracing was kept the same as the receivers spacing i.e., 12.5 m. The inversion grid spacing is 300 m in the horizontal direction and 50 m in the vertical direction. Each inversion run was required to converge to a minimum misfit and the procedure was carried out until no further update was obtained in the velocity model of two consecutive iterations of the inversion. The final velocity model obtained by TTT after 14 iterations (shown in Figure 5b), where χ^2 was reached to 1.2

in comparison to the initial χ^2 of 1200, a high initial χ^2 is a result of choosing initial velocity model. The final velocity model may not represent the true sub-surface velocities until there is sufficient ray coverage and two-way travel time residuals reduction.

The ray coverage could be measured by the parameter derivative weight sum (DWS) (Van Avendonk et al., 2004), the DWS diagram is shown in Figure S2b. The ray coverage diagram is obtained by the derivative weight sum parameter, which is the sum along all columns of the Fretchet matrix of first derivatives (Van Avendonk et al., 2004). The initial (blue) and final (red) residuals plot shown in Figure S2a to further validate our tomography results. The final travel-time residuals reach ~16 ms, close to the uncertainty assigned to the data of 15 ms for tomographic inversion. We could see that the residuals decrease for the whole region (Figure S2a), except at the 160-180 and 310-320 km there are higher residuals than the rest of the profile, it could be a result of the sill intrusion at those places which could have impacted the travel time picking. The cyan line in the tomographic velocity model has been shown in the well-resolved regions, which corresponds to regions having sufficiently high ray coverage (Figure S2b). The velocity near the seabed could be a result of smoothing because only first pass of DC was applied and rays could not have converged in the topmost sedimentary layer. We constrained velocity down to ~5 km depth along the profile (cyan line in Figure 5b), which enables us to measure the velocity of the sedimentary sequence from seafloor to the Paleocene period (1.8 – 4.2 km/s) that is in good agreement with the velocity obtained in Mackenzie et al. (2002) and we also constrained the velocity of VR1 and VR4 (4.5-4.8 km/s). VR2 and VR3 are below the resolution of the TTT and considered to be of same velocity as VR1 and VR4 in gravity modelling for density computation.

5. Gravity and magnetic modelling

The forward modelling involves constraining the geological model with petrophysical values which are used to compute the geophysical response of the model. The initial geological model is changed to obtain a better fit between calculated and observed gravity and magnetic data. The final potential field model is non-unique as the field can be fitted by many possible models, which includes those that are geologically non-realistic. Hence, to avoid building a non-realistic geological model, the PSTM seismic profile is used to constrain the shallow sedimentary structures to top of the crystalline basement. The crystalline basement is constructed using prior information on the crustal thickness and the Moho depth from nearby wide-angle seismic profiles in the Rockall Basin (Hauser et al. 1995; O'Reilly et al. 1996; Readman et al. 2005; Kimbell et al. 2010).

Gravity and magnetic modelling are performed using the software Geosoft GM-SYS of Seequent. To build an initial geological model the seismic horizons from the time migrated seismic section were picked from the seabed to the top of the basement. Seismic time of sedimentary sequence is converted to depth by using the velocity obtained from TTT (see section 4). The post-rift sedimentary sequences are well constrained in the velocity models from the TTT down to a depth of 5 km and the velocity of the Cretaceous sedimentary sequence was used from (Mackenzie et al. 2002). The crystalline basement and upper mantle velocity was used from wide-angle seismic refraction data (O'Reilly et al. 1996, Morewood et al. 2005).

After building the initial geological model, the mean velocities of the seismic stratigraphic layers and basement were converted into mass density (Tomar et al. 2022).

The classical velocity to density conversion Nafe-Drake curve (Ludwig et al. 1970) encompasses the entire velocity range encountered in this work. This V_p and density relationship is as below:

$$\rho = 1.6612V_p - 0.4721{V_p}^2 + 0.0671{V_p}^3 - 0.0043{V_p}^4 + 0.000106{V_p}^5. \quad (1)$$

where, V_p is the P-wave velocity in km/s and ρ is the density in g/cm^3. This relationship is used to convert the velocity to density for the crystalline crust. The Hughes et al. (1998) relationship (eq.2) is used for the post and syn-rift sediments, as it is based on exploration well log from FSB, which has similar sedimentary sequences to the Rockall Basin:

$$\rho = 0.295 + 1.337V_p - 0.273{V_p}^2 + 0.019{V_p}^3. \quad (2)$$

The geometries of the Moho are estimated through a "trial-and-error" method, which consisted of modifying the geometry of these deeper interfaces, while keeping the sedimentary sequence and two layers crust fixed until the calculated free-air gravity anomaly fits well with the observed gravity anomaly.

Two crustal layers beneath the sediments were defined based on the crustal structure in Ireland and Britain (O'Reilly et al., 1996, 2012; Morewood et al. 2005). The upper crustal layer has a velocity of ~6.1 km/s, and the lower crustal layer of ~6.8 km/s. The software uses the method for computation of the gravity and magnetic model is based upon Talwani et al. (1959) and Talwani and Heirtzler (1964) and it uses the algorithms described in Won and Bevis (1987). Figure 6d shows all horizons in time (Picked from seismic section, Figure 4), whereas depth converted horizons are shown in Figure 6c. Using the geological model obtained from seismic data and two-layer crystalline crust, defined by the nearby crustal model, the Moho is adjusted until a good match between observed and calculated gravity data is achieved (6b).

The properties of the model change with depth (in the Z direction) and in the direction of the profile (X direction). In the GM-SYS software, the models are extended to 30,000 km in the ±X directions, also to 50 km in depth to eliminate edge-effects. The velocity of the structures identified as the BVRS (Scrutton and Bentley, 1988) in the seismic section (Figure 4), obtained using TTT are consistent with the basaltic intrusions, as well as with the fault blocks of crystalline basement. Hence it is important to analyze the magnetic signature of these structures to constrain the interpretation. After building the geological model for crustal to upper mantle from seismic and gravity data, the magnetic susceptibility and remanent magnetisation (RM) are assigned to the ridge like features VR1, VR2, VR3, and VR4 in the model (Figure 6a) to test the magnetic response and fit the observed and modelled magnetic fields.

Figure (6a) shows the magnetic signature for the seismic profile, black dots represent the observed magnetic data acquired by PAD during the seismic data acquisition and blue curve represents the old Verhoef et al. (1996) magnetic data. Although, the magnetic anomaly of the volcanic ridge like structures follow the same trend but due to a major difference between the two data set, the PAD magnetic data is used for the 2D magnetic modelling. A small magnetic susceptibility (0.008 SI) is introduced in the Cretaceous sediments to account for sills and lava flows. The upper crust is assigned susceptibility of 0.03 SI with a zero magnetisation assumed else-where. The magnetic susceptibility of 0.09 SI for structures VR2, VR3 and VR4 and 0.18 SI for VR4, and a value of 1A/m of RM for all these ridge like structures are introduced in the magnetic modelling. A partial explanation for the high magnetic susceptibility associated with VR1 could be that the VR1 feature is larger in size and closer to the seafloor; an effect of it also observed in gravity anomaly (Figure 6b). In the absence of the well and other physical parameters magnetic inclination and declination are calculated in the software (Geosoft) for the Rockall region and inclination of 70° and declination is -12° are used in the analysis. It could be seen that the calculated magnetic anomaly with (red curve, Figure 6a) and without (green curve, Figure 6a) introducing the remnant magnetisation (RM) satisfactorily explains the observed magnetic data. The gravity and magnetic properties for the volcanic ridges and all layers are given in Table 1.

6. Integrated geophysical results

An integrated interpretation of seismic, gravity and magnetic datasets to constrain the structure and extent of the volcanic ridges is presented in Figure 4b. The Rockall Basin comprises of generally flat sedimentary sequences from north to south (Mackenzie et al. 2002; Morewood et al. 2005), we also observed similar structures (Figure 4b). The picked horizons are indicated with black lines, the top of crystalline basement is not visible beneath the igneous intrusions, so a careful picking was carried out for the top of basement. The PAD14-028 seismic line (Figure 4a) was selected due to its unique location along the margin as it cuts perpendicularly through the NW-SE aligned volcanic ridges. The velocity model obtained by TTT follows the geological structures interpreted in the seismic section (Figure 4b). The Moho shown in Figure 4b is computed in gravity modelling (Figure 6). The combined presence of relatively high-velocity, high-magnetic anomaly and typical morphology suggests the volcanic nature of these ridge-like structures, as identified earlier in this region by Scrutton and Bentley, (1988). The volcanic ridges VR1 and VR4 are investigated in detail (Figure 7) to analyze the approximate age of these structures in the absence of the well data (Bérdi, 2022).

The NW-SE Regional Seismic Line E1 (IS6_04_E1) across northern Rockall Basin was tied to 5/22-1, 12/2/1, 12/2/2 wells (MERC, 2020). The IS6_04_E1 composite line comprises PAD13-029 and PAD14-017, to which we have correlated our seismic interpretation on PAD14-028 (Figure 2a). We have identified and correlated four key seismic horizons (unconformities/sequence boundaries): C30: Base Oligocene, C40: Intra Eocene), Base C50, and C100: Top Shetland (see Chronostratigraphic Chart in Figure 2b). However, as we move southwest along PAD14-028, the latter two seismic horizons are occasionally obscured due to the presence of igneous sill complexes, lava flow, and volcanic ridges.

These saucer shaped sill complexes have been named as the Atlantic Margin Sill Complex by Schofield et al. (2018). Discontinuous Anomalously high-seismic amplitudes on either side of VR1 was interpreted as lava flow, following lava flow seismic facies analysis (Planke et al. 2017). We observe forced folded structures due to the intrusion of the volcanic structure VR4 as well as due to sill intrusions within the Paleocene sequence. Similar deformational forced folding structures associated with volcanic ridge and lava flow are shown in Supplementary Figure S3.

The gravity modelling and seismic section provide the crustal to upper mantle model beneath the southern Rockall Basin that broadly agrees with the independent estimates using gravity inversion methods (Welford et al. 2010). The Moho depth, extracted from a grid obtained using 3D gravity inversion (Welford et al. 2010, 2012) is superimposed over the Moho obtained in this study (Figure 8). A good overall correlation between two results is present even though the input data (e.g., sediment thickness) and parameterization in two methods are different. The maximum difference between these two results is 1.7 km, which is within the uncertainty considered (±2 km) in the crustal thickness (Figure 9a) for computing the stretching factor.

The depth converted basement from the PSTM and the calculated Moho from gravity modelling permits computation of the crustal thickness (Figure 9a). Based on the crustal thickness, we could compute the bulk stretching factor β ($\beta = T_0/T_C$, -with T_0 the initial crust thickness and T_C the “stretched” crustal thickness). The initial crustal thickness of 30 km is used for the Rockall Basin based on previous studies (Landes et al. 2005; O’Reilly et al. 2012). Figure 9b shows the observed stretching factor β with a ±2 km uncertainty in the crustal thickness estimation. The observed crustal thickness in the southern Rockall Basin is in good agreement with Shannon et al. (1999), Welford et al. (2012) and Funck et al. (2017a, b). A maximum stretching factor $\beta > 6$ is observed (Figure 9b) beneath the BVRS and further south values of $\beta > 3$ are obtained. According to 1-D numerical simulations (Pérez-Gussinyé and Reston, 2001), if the value of the bulk stretching factor (β) exceeds 3 (which is required to achieve the full crustal embrittlement), then it promotes low-temperature mantle serpentinisation. But a recent study (Liu et al. 2022) suggest that the detachment like structures is formed by full crustal embrittlement and the active faults bifurcate into brittle and ductile deformation.

The earlier work of Scrutton and Bentley (1988) suggested that the high gravity anomaly between the volcanic ridges VR2 and VR3 could be a result of the crustal thinning. It could also be explained with an underlying mafic intrusion in the crystalline basement. The results of our study show that the gravity anomaly pattern in the region is not reconcilable with this possibility (Figure S4) but is most compatible with more recent nearby wide-angle seismic studies (Morewood et al., 2005). Figure S4 shows two scenarios of gravity modelling, one with mantle serpentinisation (green curve) using the gravity model (Figure S4b), it shows that a serpentinised mantle layer does not change the modelled anomaly (red curve obtained in Figure 6). Secondly, if a mafic intrusion replaces the serpentinised mantle layer (Figure S4c) the modelled gravity anomaly (blue curve in Figure S4a) cannot explain the observed gravity anomaly.

7. Discussion

The earlier work of Scrutton and Bentley, (1988) identified three large NW-SE striking curvilinear ridges as the BVRS in the Irish southern Rockall Basin. Several studies including the most recent Horni et al. (2017) identified these curvilinear ridges as igneous centres. In this paper, we identified four ridge-like structures similar to those identified by Scrutton and Bentley, (1988). The velocity of these structures obtained by using TTT is 4.5-4.8 km/s, which is typical but not diagnostic on basaltic rocks. Alternatively, a sedimentary horst/ridge overlaid by thinner lava flows could "blur" the underlying imaging and also explain the magnetic signature. But due to the morphology of these structures, the seismic velocity and high magnetic signature (~400 nT), they are interpreted as a volcanic ridge system, comprising the BVRS (Scrutton and Bentley, 1988). The volcanic ridge structures VR1 - VR4, and associated saucer-shaped igneous sill complexes and lava flows are associated with the forced folded structures in the sedimentary layers and draping on the flanks of the interpreted volcanic ridges. (Figure 7).

Forced folding induced by saucer-shaped igneous sill complexes are also observed in close association with the volcanic ridges. The forced folds form through continual growth and are directly linked to the mechanical emplacement of the underlying saucer-shaped igneous sills, and are related to an increase in faulting and deformation of the overlying strata (Hansen and Cartwright, 2006). The volcanic system needs a feeder-zone to break through the crust and emplace the volcanic ridges in the basin.

However, the seismic profile fails to image the deeper faults or the magma source due to heavy sill flooding. Moreover, the orientation of the seismic profile is parallel to the fault strike direction, making them difficult to image. Pre-existing rift related faults, which could be magma feeding pathways has been demonstrated in the upper Paleozoic to Mesozoic succession in the central part of the Rockall Basin (Figure 15a; Stoker et al. 2017). Basaltic lava flows and igneous sills are closely emplaced with the volcanic ridge system, with the magma source being hidden much deeper, as suggested by Scrutton and Bentley, (1988).

The accurate timing of the magmatic event, i.e., the timing of emplacement of the genetically related igneous saucer-shaped sill complexes and volcanic ridges can be constrained by dating strata that onlap the forced-folds or the volcanics. In the absence of actual dating and well data, we make an attempt to infer the approximate time period during which the volcanic ridges and associated sills and lava flow were emplaced. A detailed seismic-well study of the Irish Rockall Basin igneous sill complex along the northeastern slope of Rockall Basin revealed that the emplacement of igneous intrusions and associated forced folding initiated at the end of Maastrichtian and lasted for ca. 15 Ma, before ceasing near the end of Ypresian (Magee et al. 2014).

Compound folds are observed throughout the Paleocene-to-Middle Eocene, above stacked interconnected igneous sill complexes (Magee et al., 2014). This is consistent with our seismic interpretation, with all the igneous sill complexes beneath the Base C50 unconformity (~50Ma, Figure 2b). This is further supported by the evidence of lava flows, beneath the C100-Top Shetland unconformity (~62-63 Ma) and within the Paleocene sedimentary sequence, draping VR1 (Figure 7c). Additionally, we observed lava flows underlying the C100-Top Shetland unconformity, within the Paleocene sedimentary sequence, which is associated with an identical volcanic ridge, (Supplementary Figure S3) which could be a continuation of VR2 interpreted in this study.

By observing the deformed nature of the Base C50 and C40-Intra-Eocene unconformities, we infer that the lava flow might have occurred at the Paleocene-Eocene transition. Folded structures associated these volcanic ridges, are also present and sometimes occur with lava flows on PAD13 and PAD14 seismic profiles in the southern Rockall Basin within the BVRS region outlined by Horni et al., (2017). It is evident these volcanic features are part of the NAIP, with VR2-VR4 are aligned with the volcanic ridges identified by Scrutton and Bentley (1988).

However, the inclusion of VR1 within the BVRS is debatable. Based on the location of strong positive magnetic anomalies, Keen et al., (2014) had illustrated volcanic features in Rockall Basin, those which appear to be conjugate to the Charlie Gibbs Volcanic Province. VR1 is located to the south of the western most NW-SE aligned volcanic province in the Rockall Basin (Figure 11 of Keen et al., 2014), which could be part of the Rockall Bank volcanic province. However, the morphology of the volcanic ridge and induced deformation (S3- supplementary Figure) resembles that of VR1 and prompts us to infer that they are part of the BVRS. The volcanic ridge (S3 supplementary Figure) is part of the SW-NE trending volcanic province of the BVRS as illustrated in Fig 11 of Keen et al., (2014).

The episodic volcanism (from the Late Cretaceous to the Mid-Eocene) that formed the igneous edifices situated on extended continental crust in the Rockall region was linked to the Iceland plume pulsations which may have occurred at 5–10 myr intervals (O'Connor et al., 2000) and could have even shorter pulsations (White and Lovell, 1997; Poore et al. 2009). Large seamounts were formed on the Rockall plateau and in the Rockall Basin around 52 Ma, and the Iceland plume activity increased at 55 and 52 Ma, which could indicate that the Early Eocene SOIF (seamount-like oceanic igneous features) formation in the NE Atlantic may have resulted from higher than usual mantle plume activity (Gaina et al., 2017).

The proto-North Atlantic experienced a long period of extension from the Late Paleozoic and throughout the Mesozoic. Figure 9 of (Horni et al., 2017) shows the Cretaceous stratigraphic distribution reconstructed to 80Ma (Stoker et al., 2017), by highlighting the lithospheric thinning pattern prior to the arrival of the plume beneath Greenland. Material is preferentially channeled into the Rockall–Hatton margins as a consequence of the pre-existing lithospheric configuration. As suggested by Horni et al. (2017), closer proximity of the Rockall-Hatton region to the site of the impacting plume probably led to it being the preferred region for lateral flow of plume material.

In this study we have observed lithospheric thinning beneath the BVRS, where the stretching factor is > 6 (Figure 9b). This observation along with the evidence of Iceland plume activity in the northern Irish Rockall Basin (O’Connor et al., 2000), we are prompted to believe that the Icelandic plume had an impact on the volcanic ridges identified in this study. However, the link between widespread igneous activity and late-syn-rift and earliest seafloor spreading in the NE Atlantic region cannot be completely ruled out (Skogseid et al., 2000; Gernigon et al. 2004). In a recent study volcanism in the Hatton Basin is observed during the Paleocene-Eocene transition as well from C100-C50 at 62-52 Ma (Bérdi, 2022). The exact age of the BVRS cannot be determined until these volcanic ridges are drilled for dating. Our results show that the ridges in the Rockall Basin are of ~ 3 km thick, the depth being uncertain due to poor seismic reflections observed within the volcanic ridges.

Figure 10 shows the 1D modelling results (based upon Bown and White, 1995), with contours of syn-rift melt produced during the rifting for cool lithosphere with the varying rift-duration and stretching factor. The rifting must be of noticeably short period (~< 10 Ma) to produce a ~3 km of melt for the stretching factor of >6 in the Rockall Basin (Figure 10). However, it is less likely for the Rockall Basin that a rifting period would be as short as ~10 Ma. The rift duration of the Rockall Basin is estimated 20-60 Ma (Pérez-Gussinyé et al. 2001; Pearse, 2002). This 1D calculation suggests that very little, or no syn-rift melt is generated for a rift duration of 20-40 Ma (green box, Figure 10). The integrated geophysical data analysis suggests that pre-existing crustal and lithospheric structure prior to the North Atlantic opening played a crucial role in the emplacement of the BVRS basalt features (igneous sills and volcanic ridges), at a later stage (Paleocene to Mid-Eocene), than previously thought.

8. Conclusions

Constrained 2-D gravity forward gravity modelling of the free air data over a 2D multichannel seismic profile was performed and a regional density anomaly model was generated by using velocity analysis and a-priori knowledge, combined with a detailed seismic stratigraphic interpretation. An independent proxy for Moho structure was obtained by defining a density anomaly and this information was combined with available sediment thickness estimates to facilitate the investigation of crustal thickness as well as variations in the degree of extension along the profile. Our key findings include:

1. The velocity of sedimentary sequences in the Rockall Basin varies between 1.8 to 4.5 km/s on the seismic profile adjacent to the western slope of the basin. The velocity of the volcanic ridges (VR1 and VR4) falls in the range 4.5-4.8 km/s. The

velocity along with the morphology of the volcanic ridges and high magnetic anomaly suggest that they are possibly composed of basalt and basaltic ash.

2. The crustal thickness beneath the BVRS is observed to be as thin as <~ 4 km, that in turn results the stretching factor to be >6. Mafic intrusion would not explain the high gravity anomaly beneath VR2 and VR3. The high gravity anomaly in the middle of the basin could be related to crustal thinning.
3. We interpreted four volcanic ridges emplaced in the Paleocene-Eocene sequence, in the south of the Rockall Basin, which are part of the BVRS. Based on seismic evidence, we further suggest that these volcanic ridges could be intrusive in nature and could be a result of the interaction of the Icelandic Plume with the continental crust beneath the Rockall Basin. Based upon the stretching-factor analysis, we could infer that the pre-existing thin lithosphere and crust beneath the BVRS facilitated the channeling of Iceland plume magma to form these volcanic centres.

1) Table 1.

S. N.	Geological layer	P-wave velocity (m/s)	Density (g/cm^3)	Susceptibility (SI)	Remanent Magnetisation (A/m)	Inclination/ Declination
1	Water	1500	1.03	0	0	
2	Oligocene-Present	2000	2.2	0	0	
3	Eocene	2800	2.34	0	0	
4	Paleocene	3800	2.41	0	0	
5	Cretaceous	4900	2.54	0.008	0	
6	VR1, VR2, VR3	4800	2.52	0.09	1	70/-12°
7	VR4	4800	2.52	.18	1	70/-12°
8	Upper crust	6100	2.7	0.03	0	
9	Lower crust	6800	2.85	0	0	
10	Mantle	8100	3.34	0	0	
11	Serpentinised mantle	7700	3.28	0	0	
12	Ultra-mafic igneous rocks	7200	2.99	0	0	

Table 1. Parameters of each layer used in the seismic interpretation and gravity modelling.

References

Archer, S.G., Bergman, S.C., Iliffe, J., Murphy, C.M. & Thornton, M. (2005). Palaeogene igneous rocks reveal new insights into the geodynamic evolution and petroleum potential of the Rockall Trough, NE Atlantic Margin. Basin Research, **17**, 171–201.

Arnulf, A., Singh, S., Harding, A., Kent, G., & Crawford,W. (2011). Strong seismic heterogeneity in layer 2a near hydrothermal vents at the Mid-Atlantic Ridge. Geophysical Research Letters, 38, L13320. https://doi.org/10.1029/2011GL047753

Audhkhasi, P., & Singh, S. C. (2019). Seismic structure of the upper crust from 0–75 Ma in the equatorial Atlantic Ocean on the African plate using ultralong offset seismic data. Geochemistry, Geophysics, Geosystems, 20(12), 6140-6162.

Bentley, P. A. D. (1986). Geophysical studies in southern and central Rockall Trough, northeast Atlantic. KB Thesis Scanning Project.

Bérdi L., (2022). An integrated study of the Hatton Basin: its role in regional North Atlantic development. Ph.D. Thesis; university College Dublin.

Berryhill, J. R. (1984). Wave-equation datuming before stack. Geophysics, 49(11), 2064–2066.

Bown, J. W., & White, R. S. (1995). Effect of finite extension rate on melt generation at rifted continental margins. Journal of Geophysical Research: Solid Earth, 100(B9), 18011–18029.

Broadley, L., Schofield, N., Jolley, D., Howell, J., and Underhill, J. R., (2020), UK Rockall Prospectivity: Re-awakening exploration in a frontier basin: Petroleum Geoscience, p. petgeo2019-2098.

Burov, E. & Gerya, T, (2014). Asymmetric three-dimensional topography over mantle plumes. Nature **513**, 85–89.

Celli, N. L., Lebedev, S., Schaeffer, A. J., & Gaina, C. (2021). The tilted Iceland Plume and its effect on the North Atlantic evolution and magmatism. Earth and Planetary Science Letters, 569, 117048.

Cole, J.E. & Peachey, J. (1999). Evidence for pre-Cretaceous rifting in the Rockall Trough: an analysis using quantitative plate tectonic modelling. In: Fleet, A.J. & Boldy, S.A.R. (eds) Petroleum Geology of Northwest Europe: Proceedings of the 5th Conference. Geological Society, London, 359–370, https://doi.org/10.1144/0050359.

Doré, A.G., Lundin, E.R., Jensen, L.N., Birkeland, Ø., Eliassen, P.E., and Fichler, C., (1999). Principle tectonic events in the evolution of the Northwest European Atlantic margin: Petroleum Geology of Northwest Europe; proceedings of the 5th conference, v. 5, p.41-61.

Ebinger, C. J. & Sleep, N. H., (1998). Cenozoic magmatism throughout east Africa resulting from impact of a single plume. Nature **395**, 788–791.

England, R.W. & Hobbs, R.W., (1997). The structure of the Rockall Trough imaged by deep seismic reflection profiling, Journal of the Geological Society, London, **154**, 497-502.

Funck, T., Erlendsson, Ö., Geissler, W. H., Gradmann, S., Kimbell, G. S., McDermott, K., & Petersen, U. K. (2017a). A review of the NE Atlantic conjugate margins based on seismic refraction data. Geological Society, London, Special Publications, 447(1), 171–205.

Funck, T., Geissler, W. H., Kimbell, G. S., Gradmann, S., Erlendsson, Ö., McDermott, K., & Petersen, U. K. (2017b). Moho and basement depth in the NE Atlantic Ocean based on seismic refraction data and receiver functions. Geological Society, London, Special Publications, 447(1), 207–231.

Gaina, C., Blischke, A., Geissler, W.H., Kimbell, G.S., Erlendsson, Ö., (2017). Seamounts and oceanic igneous features in the NE Atlantic: a link between plate motions and mantle dynamics. Geological Society, London, Special Publications 447, 419-442.

Geotrace Technologies Ltd. (2015). Processing of 2D seismic data. Long offset survey – Atlantic margin, offshore Ireland, 43 p.

Gernigon, L., Ravaut, C., Shannon, P. M., Chabert, A., O'Reilly, B. M., & Readman, P. W. (2004). Contrasting styles between the structure and the magmatism of the West and South Hatton/Rockall Margins (North Atlantic Igneous Province). AGU Fall Meeting Abstracts, 2004, V51B-0567.

Ghosal, D., S. Singh, and J. Martin (2014), Shallow subsurface morphotectonics of the nw sumatra subduction system using an integrated seismic imaging technique, Geophysical Journal International, 198 (3), 1818–1831, doi:10.1093/gji/ggu182.

Hansen, D. M., & Cartwright, J. (2006). The three-dimensional geometry and growth of forced folds above saucer-shaped igneous sills. Journal of Structural Geology, 28(8), 1520-1535.

Hauser, F., O'Reilly, B. M., Jacob, A. W. B., Shannon, P. M., Makris, J., & Vogt, U. (1995). The crustal structure of the Rockall Trough: differential stretching without underplating. Journal of Geophysical Research: Solid Earth, 100(B3), 4097–4116.

Holford, S. P., Green, P. F., Duddy, I. R., Turner, J. P., Hillis, R. R., & Stoker, M. S. (2009). Regional intraplate exhumation episodes related to plate-boundary deformation. Geological Society of America Bulletin, 121(11–12), 1611–1628.

Hopper, J. R., Dahl- Jensen, T., Holbrook, W. S., Larsen, H. C., Lizarralde, D., Korenaga, J., Kent, G. M., & Kelemen, P. B. (2003). Structure of the SE Greenland margin from seismic reflection and refraction data: Implications for nascent spreading center subsidence and asymmetric crustal accretion during North Atlantic opening. Journal of Geophysical.

Horni, J. Á., Hopper, J. R., Blischke, A., Geisler, W. H., Stewart, M., McDermott, K., ... & Árting, U. (2017). Regional distribution of volcanism within the North Atlantic Igneous Province. Geological Society, London, Special Publications, 447(1), 105-125.

Howell, S. M. et al. (2014). The origin of the asymmetry in the Iceland hotspot along the Mid-Atlantic Ridge from continental breakup to present-day. Earth and Planetary Science Letters **392**, 143–153.

Hughes, S., Barton, P., & Harrison, D. (1998). Exploration in the Shetland-Faeroe Basin using densely spaced arrays of ocean-bottom seismometers. Geophysics, 2, 490–501.

Huot, G., & Singh, S. C. (2018). Seismic Evidence for Fluid/Gas Beneath the Mentawai Fore-Arc Basin, Central Sumatra. Journal of Geophysical Research: Solid Earth, 123(2), 957-976.

Moser, T., Nolet, G., & Snieder, R. (1992). Ray bending revisited. Bulletin of the Seismological Society of America, 82(1), 259–288.

Johansson, L., Zahirovic, S., & Müller, R. D. (2018). The interplay between the eruption and weathering of large igneous provinces and the deep- time carbon cycle. Geophysical Research Letters, 45(11), 5380–5389.

Jolley, D. W., Millett, J. M., Schofield, N., & Broadley, L. (2021). Stratigraphy of volcanic rock successions of the North Atlantic rifted margin: the offshore record of the Faroe–Shetland and Rockall basins. Earth and Environmental Science Transactions of the Royal Society of Edinburgh, 112(2), 61-88.

Jones, S.M., White, N., Clarke, B.J., Rowley, E., and Gallagher, K., (2002). Present and past influence of the Iceland Plume on sedimentation, in Doré et al., eds., Exhumation of the

North Atlantic Margin: Timing, Mechanisms and Implications for Petroleum Exploration: Geological Society, London, Special Publications, v. 196, p. 13–25.

Joppen, M. & White, R.S. (1990). The Structure and Subsidence of Rockall Trough From Two-Ship Seismic Experiments, Journal of Geophysical Research, **95**, 19,821-19,837.

Keen, C. E., Dafoe, L. T., & Dickie, K. (2014). A volcanic province near the western termination of the Charlie- Gibbs Fracture Zone at the rifted margin, offshore northeast Newfoundland. Tectonics, 33(6), 1133-1153.

Kimbell, G. S., Ritchie, J. D., & Henderson, A. F. (2010). Three-dimensional gravity and magnetic modelling of the Irish sector of the NE Atlantic margin. Tectonophysics, 486(1-4), 36-54.

Koptev, A. et al. (2016). Contrasted continental rifting via plume-craton interaction: Applications to Central East African Rift. Geoscience Frontiers **7**, 221–236.

Kristoffersen, Y. (1978). Sea-floor spreading and the early opening of the North Atlantic. Earth and Planetary Science Letters, 38(2), 273–290.

Landes, M., Ritter, J. R. R., Readman, P. W., & O'Reilly, B. M. (2005). A review of the Irish crustal structure and signatures from the Caledonian and Variscan Orogenies. Terra Nova, 17(2), 111–120.

Liu, Z., Pérez-Gussinyé, M., Rüpke, L., Muldashev, I. A., Minshull, T. A., & Bayrakci, G. (2022). Lateral coexistence of ductile and brittle deformation shapes magma-poor distal margins: An example from the West Iberia-Newfoundland margins. Earth and Planetary Science Letters, 578, 117288.

Ludwig, W. J., J. E. Nafe, and C. L. Drake (1970). Seismic refraction, in The Sea, A. E. Maxwell (Editor), Vol. 4, Wiley-Interscience, New York, 53–84.

Lymer, G., Childs, C., & Walsh, J. (2022). Punctuated propagation of a corrugated extensional detachment offshore Ireland. Basin Research. https://doi.org/10.1111/bre.12745

Mackenzie, G. D., Shannon, P. M., Jacob, A. W. B., Morewood, N. C., Makris, J., Gaye, M., & Egloff, F. (2002). The velocity structure of the sediments in the southern Rockall Basin: results from new wide-angle seismic modelling. Marine and Petroleum Geology, 19(8), 989-1003.

Magee, C., Jackson, C. L., & Schofield, N. (2014). Diachronous sub- volcanic intrusion along deep- water margins: Insights from the Irish Rockall Basin. Basin Research, 26(1), 85-105.

Martos, Y. M., Jordan, T. A., Catalán, M., Jordan, T. M., Bamber, J. L., & Vaughan, D. G. (2018). Geothermal heat flux reveals the Iceland hotspot track underneath Greenland. Geophysical Research Letters, 45(16), 8214–8222.

Merlin Energy Resources Consortium (MERC), 2020. The Standard Stratigraphic Nomenclature of Offshore Ireland: An Integrated Lithostratigraphic, Biostratigraphic and Sequence Stratigraphic Framework. Project Atlas. Petroleum Affairs Division, Department of Communications, Climate Action & Environment, Special Publication 1/21.

Monahan, D. (2008). GEBCO: the second century. Looking towards a general bathymetric chart.

Morewood, N.C., Mackenzie, G.D., Shannon, P.M., O'Reilly, B.M., Readman, P.W. & Makris, J. (2005). The crustal structure and regional development of the Irish Atlantic margin region. In: Doré, A.G. & Vining, B.A. (eds) Petroleum Geology: North-West Europe & Global Perspectives — Proceedings of the 6th Petroleum Geology Conference, Geological Society, London, 1023-1033.

Naylor, D. & Shannon, P.M. (2005) The structural framework of the Irish Atlantic Margin. In: Petroleum Geology: N.W. Europe and Global Perspectives (Ed. by A.G. Dor_e & B. Vining), Proceedings of the 6th Petroleum Geology Conference, Geological Society, London, 1009–1021.

O'Connor, J., Stoffers, P., Wijbrans, J., Shannon, P., Morrissey, T. (2000). Evidence from episodic seamount volcanism for pulsing of the Iceland plume in the past 70 Myr. Nature 408, 954-958.

O'Reilly, B.M., Hauser, F., Jacob, A.W.B. & Shannon, P.M. (1996). The lithosphere below the Rockall Trough: wide-angle seismic evidence for extensive serpentinisation. Tectonophysics, 255, 1-23, doi:10.1016/0040-1951(95)00149-2.

O'Reilly, B. M., Hauser, F., & Readman, P. W. (2010). The fine-scale structure of upper continental lithosphere from seismic waveform methods: insights into Phanerozoic crustal formation processes. Geophysical Journal International, 180(1), 101–124.

O'Reilly B.M., Hauser, F., Readman, P.W. (2012). The fine-scale seismic structure of the upper lithosphere within accreted Caledonian lithosphere: implications for the origins of the "Newer Granites". Journal of the Geological Society of London, 169, 561-573.

Parnell-Turner, R., White, N., Henstock, T., Murton, B., Maclennan, J., & Jones, S. M. (2014). A continuous 55-million-year record of transient mantle plume activity beneath Iceland. Nature Geoscience, 7(12), 914–919.

Peace, A. L., Phethean, J. J. J., Franke, D., Foulger, G. R., Schiffer, C., Welford, J. K., McHone, G., Rocchi, S., Schnabel, M., & Doré, A. G. (2020). A review of Pangaea dispersal and Large Igneous Provinces–In search of a causative mechanism. Earth-Science Reviews, 206, 102902.

Peace, A. L., Welford, J. K., Geng, M., Sandeman, H., Gaetz, B. D., & Ryan, S. S. (2018). Rift-related magmatism on magma-poor margins: Structural and potential-field analyses of the Mesozoic Notre Dame Bay intrusions, Newfoundland, Canada and their link to North Atlantic Opening. Tectonophysics, 745, 24–45.

Pearse, S. (2002). Inversion and modelling of seismic data to assess the evolution of the Rockall Trough (Doctoral dissertation, University of Cambridge).

Pedersen, A., Larsen, L. M., Riisager, P. & Dueholm, K. S (2002). in The North Atlantic Igneous Province: Stratigraphy, Tectonics, Volcanic and Magmatic Processes Spec. Publ. Vol. 197 (eds Jolley, D. W, & Bell, B. R.) 157–181(Geological Society, London).

Petroleum Affairs Division of Ireland, (2006). Petroleum Systems Analysis of the Rockall and Porcupine Basins Offshore Ireland - Digital Atlas. Department of Communications, Marine and Natural Resources, Dublin, Ireland. Pages 160.

Pérez-Gussinyé, M. & Reston, T. J. (2001). Rheological evolution during extension at nonvolcanic rifted margins: onset of serpentinisation and development of detachments leading to continental breakup. Journal of Geophysical Research - Solid Earth, 106, 3961-3975, doi:10.1029/2000JB900325.

Pérez-Gussinyé, M., Reston, T. J., & Morgan, J. P. (2001). Serpentinization and magmatism during extension at non-volcanic margins: the effect of initial lithospheric structure. Geological Society, London, Special Publications, 187(1), 551-576.

Planke, S., Millett, J. M., Maharjan, D., Jerram, D. A., Abdelmalak, M. M., Groth, A., Hoffmann, J., Berndt, C., & Myklebust, R. (2017). Igneous seismic geomorphology of buried lava fields and coastal escarpments on the Vøring volcanic rifted margin. Interpretation, 5(3), SK161–SK177.

Poore, H. R., White, N., & Jones, S. (2009). A Neogene chronology of Iceland plume activity from V-shaped ridges. Earth and Planetary Science Letters, 283(1–4), 1–13.

Prada, M., Watremez, L., Chen, C., O'Reilly, B. M., Minshull, T. A., Reston, T. J., Shannon, P., Klaeschene, D., Wagner, G., & Gaw, V. (2017). Crustal strain dependent serpentinisation in the Porcupine Basin, offshore Ireland. Earth and Planetary Science Letters, 474, 148159. http://dx.doi.org/10.1016/j.epsl.2017.06.040.

Readman, P. W., O'Reilly, B. M., Murphy, T., & Makris, J. (2003). A gravity anomaly map of the Irish western seaboard. Irish Journal of Earth Sciences, 21(1), 133–142.

Readman, P. W., O'Reilly, B. M., Shannon, P. M., & Naylor, D. (2005). The deep structure of the Porcupine Basin, offshore Ireland, from gravity and magnetic studies. Geological Society, London, Petroleum Geology Conference Series, 6(1), 1047–1056.

Reston, T. J., Pennell, J., Stubenrauch, A., Walker, I., & Perez-Gussinye, M. (2001). Detachment faulting, mantle serpentinization, and serpentinite-mud volcanism beneath the Porcupine Basin, southwest of Ireland. Geology, 29(7), 587–590.

Roberts, D.G., (1975). Marine geology of the Rockall Plateau and Trough. Philosophical Transactions of the Royal Society of London, Series A 278, 447-509.

Roberts, D.G., Ginzberg, A., Nunn, K. & McQuillin, R. (1988). The structure of the Rockall Trough from seismic refraction and wide-angle reflection measurements. Nature, **332**, 632-635.

Roberts, A. M., Alvey, A. D., & Kusznir, N. J. (2019). Crustal structure and heat-flow history in the UK Rockall Basin, derived from backstripping and gravity-inversion analysis. Petroleum Geoscience, 25(2), 131-150.

Russell, M. J., & Smythe, D. K. (1978). Evidence for an early Permian oceanic rift in the northern North Atlantic. In Petrology and geochemistry of continental rifts (pp. 173–179). Springer.

Sandwell, D. T., & Smith, W. H. F. (1997). Global sea floor topography from satellite altimetry and ship depth soundings. Science, 277(5334), 1956–1962.

Sandwell, D. T., Müller, R. D., Smith, W. H. F., Garcia, E., Francis, R. (2014) New global marine gravity model from CryoSat-2 and Jason-1 reveals buried tectonic structure, Science, Vol. 346, no.5, pp. 65-67, doi:10.1126/science.1258213.

Saunders, A.D., Fitton, J.G., Kerr, A.C., Norry, M.J. &Kent, R.W. (1997). The North Atlantic Igneous Province. In: Mahoney, J.J. & Coffin, M.F. (eds) Large Igneous Provinces. American Geophysical Union, Geophysical Monograph, 100, 45–93.

Schofield, N., Jolley, D., Holford, S., Archer, S., Watson, D., Hartley, A., Howell, J., Muirhead, D., Underhill, J., and Green, P. (2018), Challenges of future exploration within the UK Rockall Basin: Geological Society, London, Petroleum Geology Conference series, v. 8, no. 1, p. 211.

Scrutton, R. A., & Bentley, P. A. D. (1988). Major Cretaceous volcanic province in southern Rockall Trough. Earth and Planetary Science Letters, 91(1-2), 198-204.

Shannon, P. M., Jacob, A. W. B., Makris, J., O'Reilly, B., Hauser, F., & Vogt, U. (1994). Basin evolution in the Rockall region, North Atlantic. First Break, 12(10).

Shannon, P.M., Jacob, A.W.B., O'Reilly, B.M., Hauser, F., Readman, P.W. & Makris, J. (1999). Structural setting, geological development and basin modelling in the Rockall Trough. In: Fleet, A.J. & Boldy, S.A.R. (eds) Petroleum Geology of Northwest Europe: Proceedings of the 5th Conference. Geological Society, London, 421–431.

Shannon, P. M. (2018). Old challenges, new developments and new plays in Irish offshore exploration. Geological Society, London, Petroleum Geology Conference series, 8(1):171.

Smythe, D.K. (1989). Rockall Trough - Cretaceous or Late Palaeozoic? Scottish Journal of Geology 25, 5-43.

Skogseid, J., Planke, S., Faleide, J.I., Pedersen, T., Eldholm, O., Neverdal, F. (2000). NE Atlantic continental rifting and volcanic margin formation. Geological Society, London, Special Publications 167, 295-326.

Steinberger, B., Bredow, E., Lebedev, S., Schaeffer, A., & Torsvik, T. H. (2019). Widespread volcanism in the Greenland–North Atlantic region explained by the Iceland plume. Nature Geoscience, 12(1), 61-68.

Stoker, M. S., Holford, S. P., Hillis, R. R., Green, P. F., & Duddy, I. R. (2010). Cenozoic post-rift sedimentation off northwest Britain: Recording the detritus of episodic uplift on a passive continental margin. Geology, 38(7), 595-598.

Stoker, M.S., Stewart, M.A., Shannon, P.M., Bjerager, M., Nielsen, T., Blischke, A., Hjelstuen, B.O., Gaina, C., McDermott, K., Ólavsdóttir, J. (2017). An overview of the Upper Palaeozoic–Mesozoic stratigraphy of the NE Atlantic region. Geological Society, London, Special Publications 447, 11-68.

Storey, M., Duncan, R. A., and Tegner, C. (2007), Timing and duration of volcanism in the North Atlantic Igneous Province: Implications for geodynamics and links to the Iceland hotspot: Chemical Geology, v. 241, no. 3, p. 264-281.

Stuart, F. M., Solveigh, L.-E., Fitton, J. G. & Ellam, R. M. (2003). High 3He/4He ratios in picritic basalts from Baffin Island and the role of a mixed reservoir in mantle plumes. Nature **424**, 57–59.

Talwani, M., & Heirtzler, J. R. (1964). Computation of magnetic anomalies caused by two dimensional structures of arbitrary shape, Computers in the Mineral Industries GA Parks, 464–480. Stanford University, Stanford, Calif.

Talwani, M., Worzel, J. L., & Landisman, M. (1959). Rapid gravity computations for two-dimensional bodies with application to the Mendocino submarine fracture zone. Journal of Geophysical Research, 64(1), 49–59.

Tomar G. & O'Reilly, B. M. (2020, August). Using Gravity based studies within north Porcupine Basin to image deep-crustal structures. Report to Irish Shelf and Petroleum Studies Group (ISPSG) of the Petroleum Infrastructure Programme (PIP).

Tomar, G., O'Reilly, B. M., Prada, M., Hardy, R., Bean, C. J., Singh, S. C., & Bérdi, L. (2022). Crustal and uppermost mantle structure of the Porcupine Basin west of Ireland from seismic and gravity methods. Marine and Petroleum Geology, 105652.

Torsvik, T. H., Mosar, J. & Eide, E. A. (2001). Cretaceous–Tertiary geodynamics: a North Atlantic exercise. Geophys. J. Int. **146**, 850–866.

Van Avendonk, H. J., Shillington, D. J., Holbrook, W. S., & Hornbach, M. J. (2004). Inferring crustal structure in the Aleutian Island arc from a sparse wide-angle seismic data set. Geochemistry, Geophysics, Geosystems, 5(8), Q08008. https://doi.org/10.1029/2003GC000664

Verhoef J, Roest W.R., Macnab R., Arkani-Hamed J & Members of the Project Team. (1996). Magnetic anomalies of the Arctic and NorthAtlantic oceans and adjacent land areas. Geological Survey of Canada.Dartmouth, Nova Scotia. Open File 3125.

Welford, J.K., Shannon, P.M., O'Reilly, B.M. & Hall, J. (2010). Lithospheric density varia ions and Moho structure of the Irish Atlantic continental margin from constrained 3-D gravity inversion. Geophysical Journal International, **183**, 79–95.

Welford, J. K., Shannon, P. M., O'Reilly, B. M., & Hall, J. (2012). Comparison of lithosphere structure across the Orphan Basin–Flemish Cap and Irish Atlantic conjugate continental margins from constrained 3D gravity inversions. Journal of the Geological Society, 169(4), 405–420.

White, N., & Lovell, B. (1997). Measuring the pulse of a plume with the sedimentary record. Nature, 387(6636), 888–891.

White, R., & McKenzie, D. (1989). Magmatism at rift zones: the generation of volcanic continental margins and flood basalts. J. Geophys. Res.94, 7685. http://dx.doi.org/10.1029/JB094iB06p07685.

Wilkinson, C.M., Ganerød, M., Hendriks, B.W.H., Eide, E.A. (2017). Compilation and appraisal of geochronological data from the North Atlantic Igneous Province (NAIP). Geological Society, London, Special Publications 447, 69.

Won, I. J., & Bevis, M. (1987). Computing the gravitational and magnetic anomalies due to a polygon: Algorithms and Fortran subroutines. Geophysics, 52(2), 232–238.

Acknowledgements

This project was funded by the Irish Centre for Research in Applied Geosciences (iCRAG), Science Foundation Ireland (SFI), Irish Shelf and Petroleum Studies Group (ISPSG) of the Petroleum Infrastructure Programme (PiP) and Dublin Institute for Advanced Studies (DIAS). This publication uses data and survey results acquired during a project undertaken on behalf of the Irish Shelf Petroleum Studies Group (ISPSG) of the Irish Petroleum Infrastructure Programme Group 4. The ISPSG comprises: AzEire Petroleum Ltd, Cairn Energy Plc, BP Exploration Operating Company Ltd, CNOOC Petroleum Europe Limited, ENI Ireland BV, Equinor Energy Ireland Limited, Europa Oil & Gas Plc, ExxonMobil E&P Ireland (Offshore) Ltd, Husky Energy, Petroleum Affairs Division of the Department of Communications, Climate Action and Environment, Providence Resources plc, Repsol Exploración SA, Sosina Exploration Ltd, Total EP, Tullow Oil Plc and Woodside Energy (Ireland) Pty Ltd.". The signal processing is done by using ECHOS software from Paradigm. We are very thankful to Dr. J. Kim Welford for providing us with the 3D Moho map of Irelands offshore. We acknowledge the Geological Survey Ireland and the Marine Institute (INFOMAR), for providing the data for this work. We also acknowledge Schlumberger for providing an academic license of Petrel software for this study. SR further acknowledges research funding from Science Foundation Ireland (SFI) and PIP. This publication derives from research supported in part by a research grant from SFI under Grant Number 13/RC/2092 and co-funded under the European Regional Development Fund and by iCRAG industry partners. Sincere thanks to Tim Minshul, Laurent Gernigon and a third reviewer for providing helpful reviews and insightful comments on the paper, which greatly improved the quality of the manuscript.

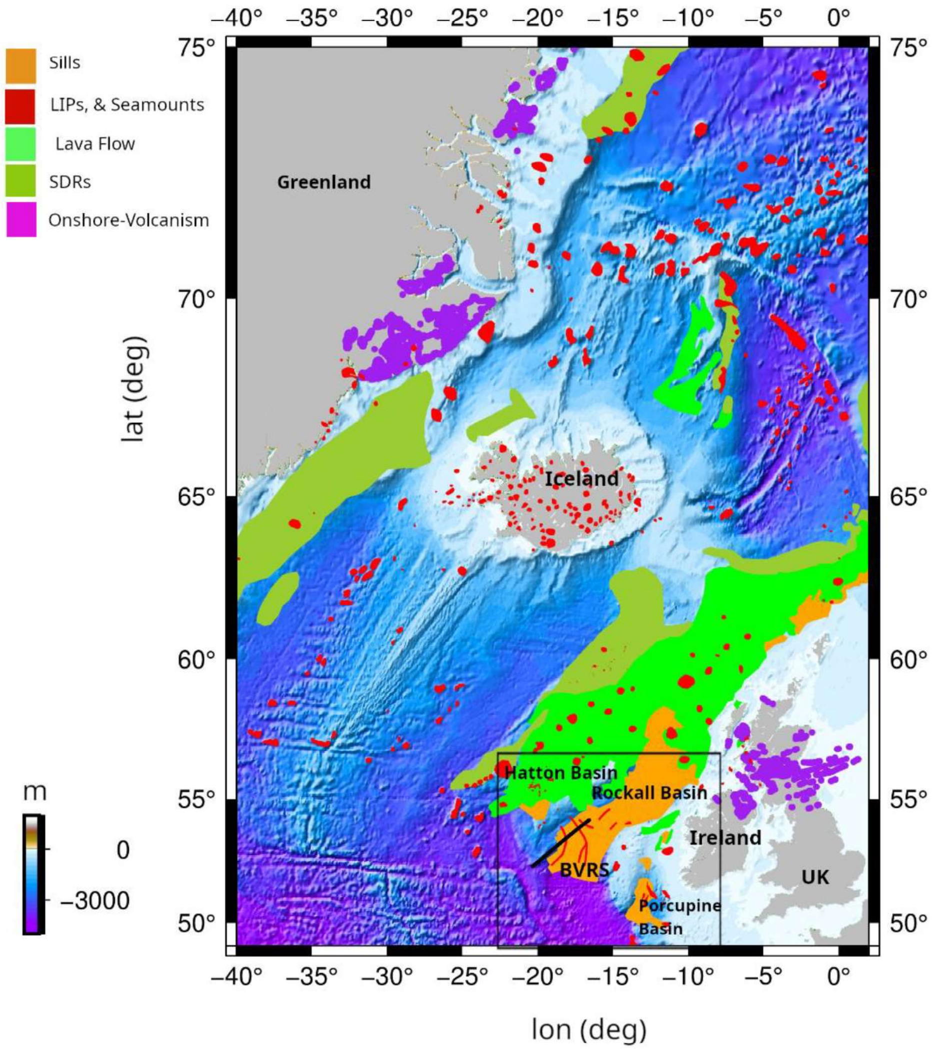

Figure 1. Topography map of the NE Atlantic region. The volcanic event in the Northeast Atlantic is shown with different colors; SDRs: (seaward-dipping reflectors, Horni et al., 2017) are shown in sea-green, onshore volcanism are shown in purple circles (Parnell-Turner et al., 2017); red polygons are seamount like oceanic igneous features (SOIF, Gaina et al., 2017) and large igneous provinces (LIP, Johansson et al., 2018). Lava flows are shown in dark-green and sill complexes are shown in orange (Horni et al. 2017; Celli et al. 2021). The SW-NE aligned black line is the location of seismic profile which is interpreted in this study. Black box represents the extent of gravity and magnetic maps Figure 3.

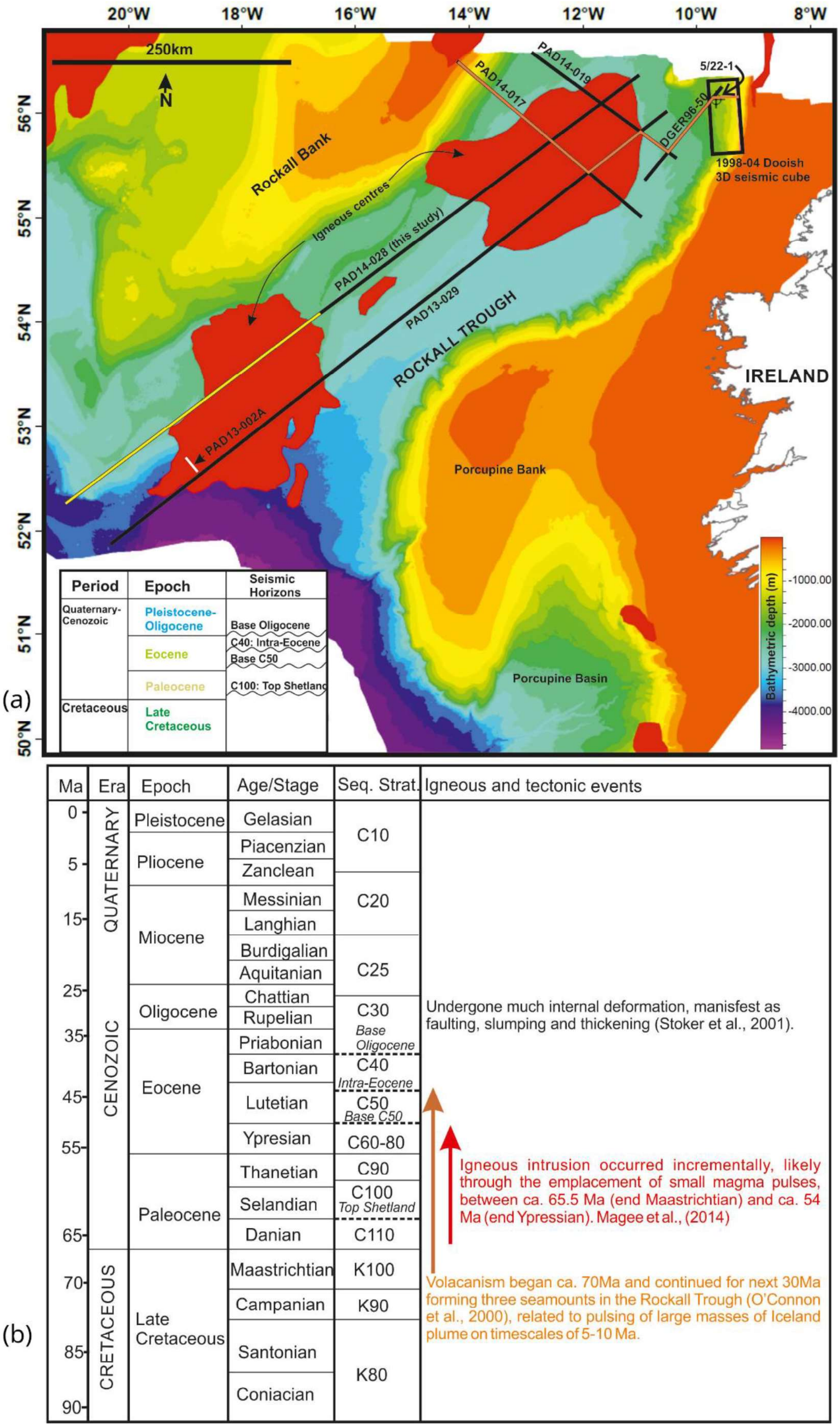
20°W
18°W
16°W
14°W
12°W
10°W
8°W
56°N
55°N
54°N
53°N
52°N
51°N
50°N
250km
N
Rockall Bank
Igneous centres
PAD14-028 (this study)
PAD13-029
PAD13-002A
ROCKALL TROUGH
PAD14-017
PAD14-019
DGER96-50
5/22-1
1998-04 Dooish
3D seismic cube
IRELAND
Porcupine Bank
Porcupine Basin
Bathymetric depth (m)
-1000.00
-2000.00
-3000.00
-4000.00
Period
Epoch
Seismic Horizons
Quaternary-Cenozoic
Pleistocene-Oligocene
Eocene
Paleocene
Cretaceous
Late Cretaceous
Base Oligocene
C40: Intra-Eocene
Base C50
C100: Top Shetland
(a)
Ma
Era
Epoch
Age/Stage
Seq. Strat.
Igneous and tectonic events
QUATERNARY
CENOZOIC
CRETACEOUS
Pleistocene
Pliocene
Miocene
Oligocene
Eocene
Paleocene
Late Cretaceous
Gelasian
Piacenzian
Zanclean
Messinian
Langhian
Burdigalian
Aquitanian
Chattian
Rupelian
Priabonian
Bartonian
Lutetian
Ypresian
Thanetian
Selandian
Danian
Maastrichtian
Campanian
Santonian
Coniacian
C10
C20
C25
C30
Base Oligocene
C40
Intra-Eocene
C50
Base C50
C60-80
C90
C100
Top Shetland
C110
K100
K90
K80
0
5
15
25
35
45
55
65
70
85
90
Undergone much internal deformation, manifest as faulting, slumping and thickening (Stoker et al., 2001).
Igneous intrusion occurred incrementally, likely through the emplacement of small magma pulses, between ca. 65.5 Ma (end Maastrichtian) and ca. 54 Ma (end Ypressian). Magee et al., (2014)
Volacanism began ca. 70Ma and continued for next 30Ma forming three seamounts in the Rockall Trough (O'Connon et al., 2000), related to pulsing of large masses of Iceland plume on timescales of 5-10 Ma.
(b)

Figure 2. (a) Five 2D seismic lines (DGER96-50, PAD14-017, PAD14-017, PAD13-029, PAD14-028), 1998-04 Dooish 3D seismic cube and 5/22-1 well locations overlain on INFOMAR bathymetric data. Regional seismic composite line (IS6_04_E1) tied to 5/22-1 well is shown as a brown NW-SE transect across the northern Rockall Basin. Please refer to MERC (2020) for detailed seismic-well tie interpretation of regional seismic composite line IS6_04_E1. Inset: Lithostratigraphic log in Rockall Basin adapted from MERC (2020). (b) A Chronostratigraphic Chart illustrating the sequence stratigraphy and key four seismic horizons interpreted (dashed lines) in this study. Igneous and volcanic events are based on O'Connor et al. (2000), Magee et al., (2014), and Wilkinson et al., (2017). The seismic profile (PAD-014_028) used in this study is indicated by yellow line in figure. The tectonic events which took place during Cretaceous to Cenozoic period are described in main text.

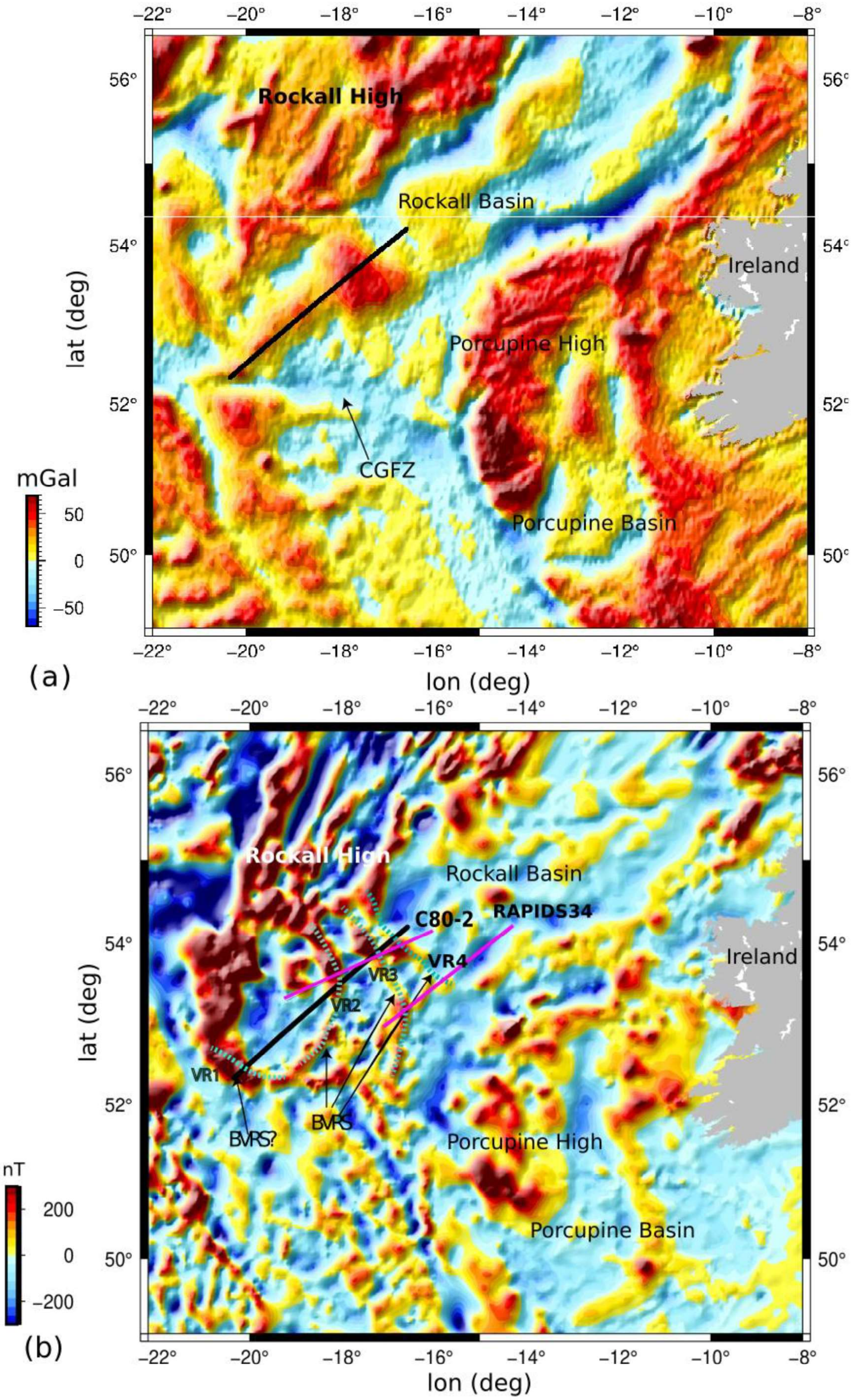
(a)
Rockall High
Rockall Basin
Ireland
Porcupine High
CGFZ
Porcupine Basin
mGal
50
0
−50
lat (deg)
lon (deg)
−22°
−20°
−18°
−16°
−14°
−12°
−10°
−8°
56°
54°
52°
50°
(b)
Rockall High
Rockall Basin
C80-2
RAPIDS34
VR4
VR3
VR2
VR1
Ireland
BVRS?
BVRS
Porcupine High
Porcupine Basin
nT
200
0
−200
lat (deg)
lon (deg)

Figure 3: (a) Free-air gravity anomaly map (Sandwell et al., 2014) of the study area. The seismic line crosses the highest gravity anomaly in Rockall Basin. (b) Magnetic anomaly map modified from (Verhoef et al., 1996); the seismic line crosses three magnetic highs (VR2, VR3 and VR4) which are part of the BVRS. A fourth magnetic high (VR1) is recognized in this study at the edge of the Charlie Gibbs Fracture Zone (CGFZ). Purple colored line in (b) indicates the location of seismic profile C80-2 used in Scrutton and Bentley, (1988) and RAPIDS34 used in (Morewood et al. 2005).

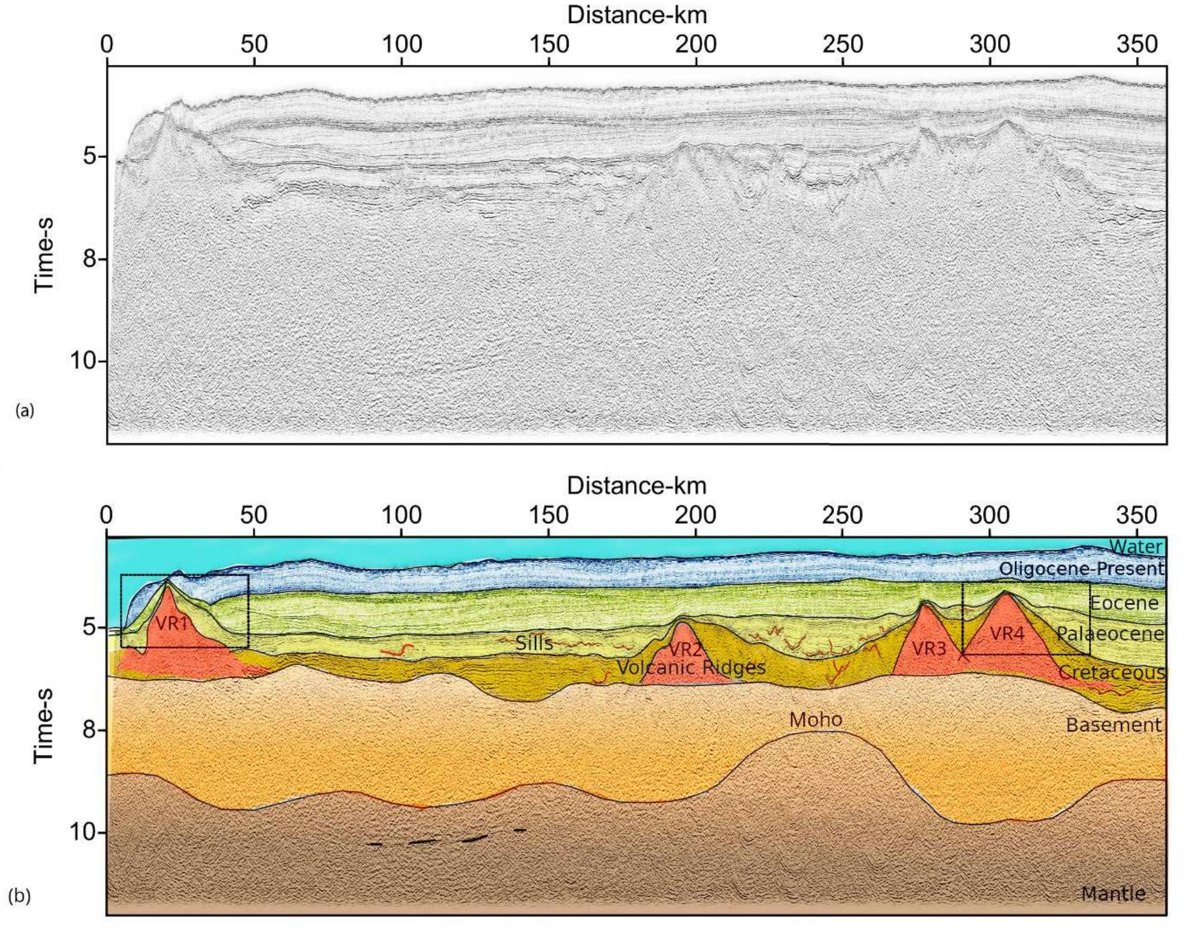

Figure 4. Pre-stack time migrated (PSTM) seismic section (a) and its interpretation (b). Black lines are the interpreted seismic horizons. Seismic reflectors are blanked beneath the volcanic structures; therefore, we used surrounding information to interpret the basement below these structures. These volcanic structures are ~ 20 km wide, intruding in Cretaceous to Paleocene sediments. The seismic resolution is limited in the crust, where gravity modelling constrains the crustal structure, with the Moho boundary determined from gravity modelling (see Figure 6). The deeper reflector ~ 10.2 s shown with the dashed line, is possibly a multiple of the Eocene-Paleocene boundary. The zoom part of the volcanic ridges indicated in black boxes are shown in Figure 7.

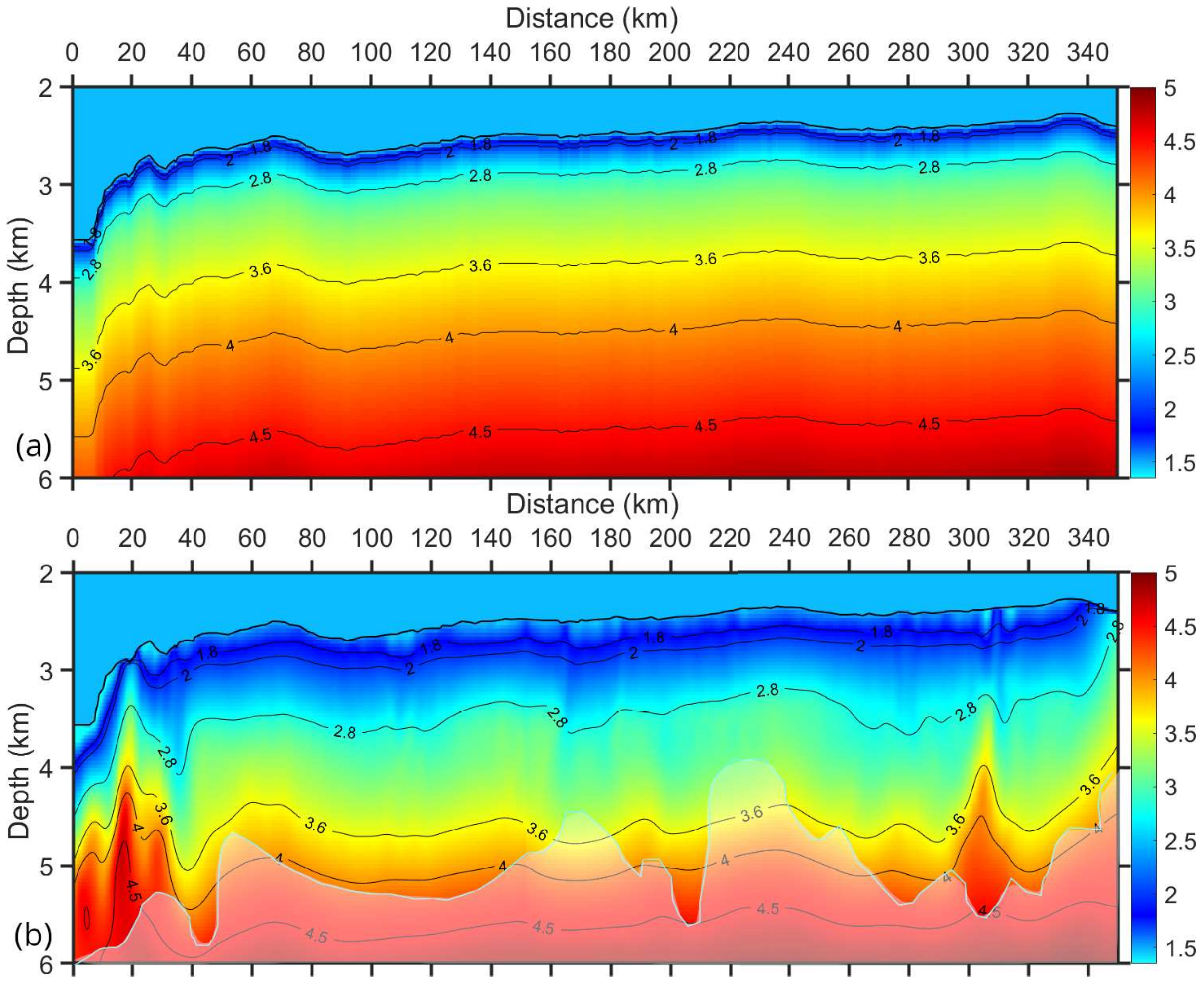

Figure 5. Velocity modelling results: (a) initial velocity model used for the tomography based on *a-priori* knowledge. (b) the final velocity model after 15 iterations. We can resolve the velocity of VR1 and VR4, because of their relatively shallow burial depth and good ray coverage down to ~5-5.5 km. The velocity of 4.5-4.8 km/s (faster than the surrounding sediments) suggests that these volcanic structures could be composed of basalt. The masked area indicates the ray coverage limit in the model (obtained from Figure S2b).

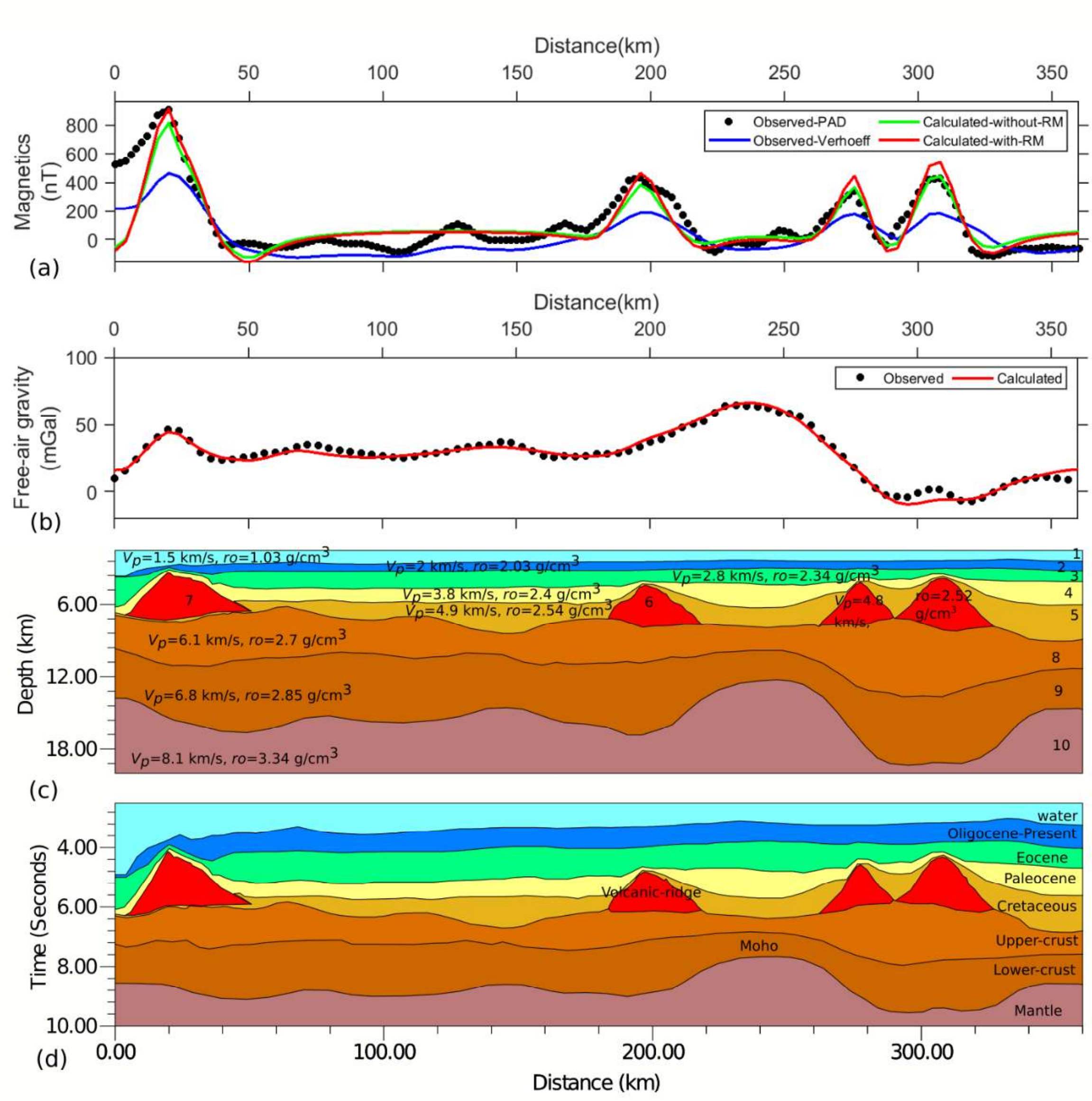

Figure 6. (a) Observed and calculated magnetic anomaly, (b) observed and calculated gravity anomaly using the depth section (c). (d) the two-way travel time of the interpreted horizons from the PSTM seismic section. The parameters (velocity, density, magnetic susceptibility and Remanent Magnetisation (RM)) used in the gravity and magnetic modelling are mentioned in Table 1. The solid black lines show all the horizons interpreted on PSTM (Figure 4b), the Moho is constrained by gravity modelling. This model closely fits the calculated gravity with the observed gravity data (b). Blue curve represents the old magnetic data (Verhoef et al. 1996), it could be seen that there is a huge difference between PAD (black dots) and the old data set (a).

The magnetic modelling shows an exceptionally good fit with the observed magnetic (PAD data) anomaly of all the four volcanic ridges (a), green curve shows the calculated magnetic model using magnetic susceptibility only, red curve represents the magnetic model with RM. We tested gravity modelling for two scenarios with partially serpentinised layer and with mafic intrusion (Figure S4) Refer to text.

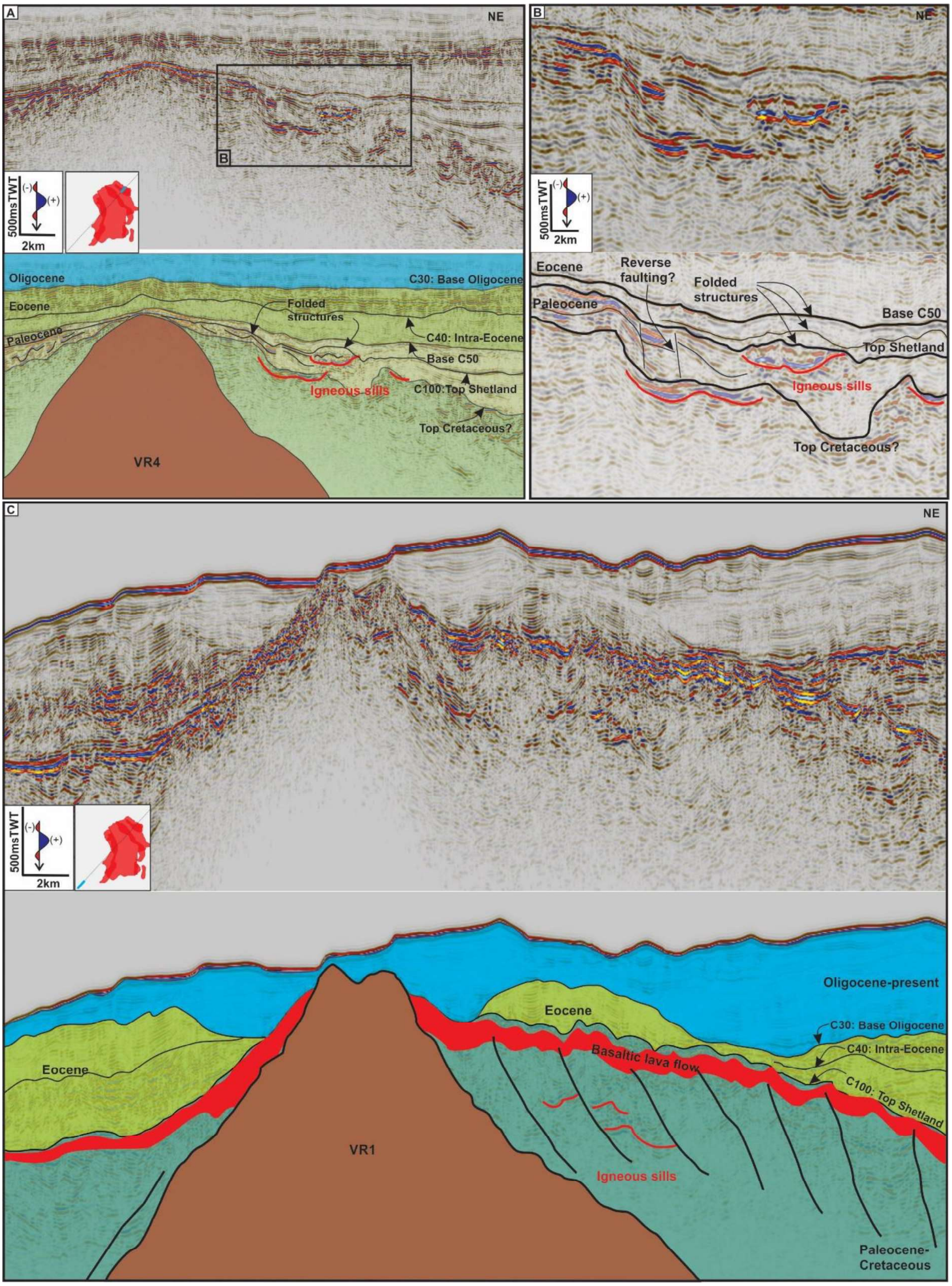
A
NE
500msTWT
(-)
(+)
2km
Oligocene
C30: Base Oligocene
Eocene
Paleocene
Folded structures
C40: Intra-Eocene
Base C50
Igneous sills
C100:Top Shetland
Top Cretaceous?
VR4
B
NE
500msTWT
2km
Eocene
Reverse faulting?
Folded structures
Paleocene
Base C50
Top Shetland
Igneous sills
Top Cretaceous?
C
NE
500msTWT
2km
Oligocene-present
Eocene
Basaltic lava flow
C30: Base Oligocene
C40: Intra-Eocene
C100: Top Shetland
VR1
Igneous sills
Paleocene-Cretaceous

Figure 7 (A) Folded Late Paleocene to early Eocene sedimentary sequence along north-eastern flank induced by the emplacement of the volcanic ridge (VR4, Figure 4) and the igneous sill complexes. These forced-folding structures are prevalent in the UK Rockall Basin (See text for discussion). (B) Zoomed part of the forced folded structures (black rectangle shown in A). Igneous intrusion induced forced folding in sedimentary layers underlying Ypresian C50 unconformity indicates that volcanic emplacement might have occurred during late Paleocene. (C) Paleocene and Eocene sediments draping basaltic lava flow, along the flanks of the volcanic ridge VR1 (Figure 4). Interpretation of Top Shetland is challenging in the southern part of the seismic line PAD14-028, due to lava flows. Refer to black rectangles for location on seismic profile (Figure 4).

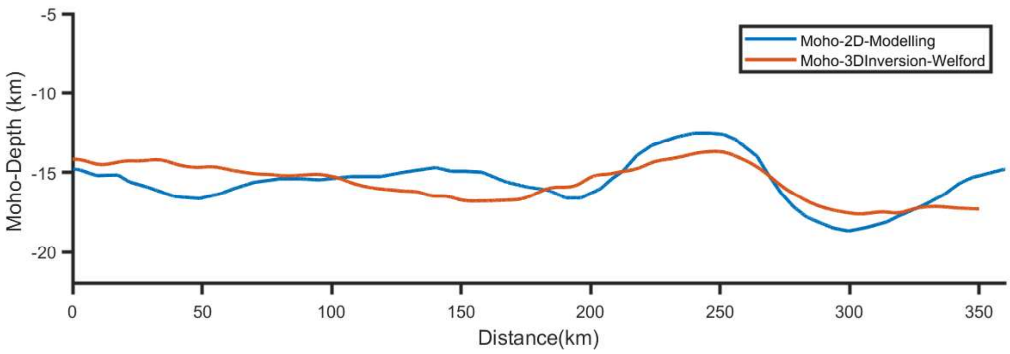

Figure 8. The Moho obtained for seismic profile used in this study is shown in blue and Moho extracted from 3D gravity inversion results (Welford et al. 2010, 2012) is shown in red. We see a good overall correlation between the Moho obtained in this study by 2D gravity modelling and in 3D gravity inversion by Welford et al. (2012). Although the difference between both the results are under 2 km uncertainty taken in computing the stretching factor. See text for discussion.

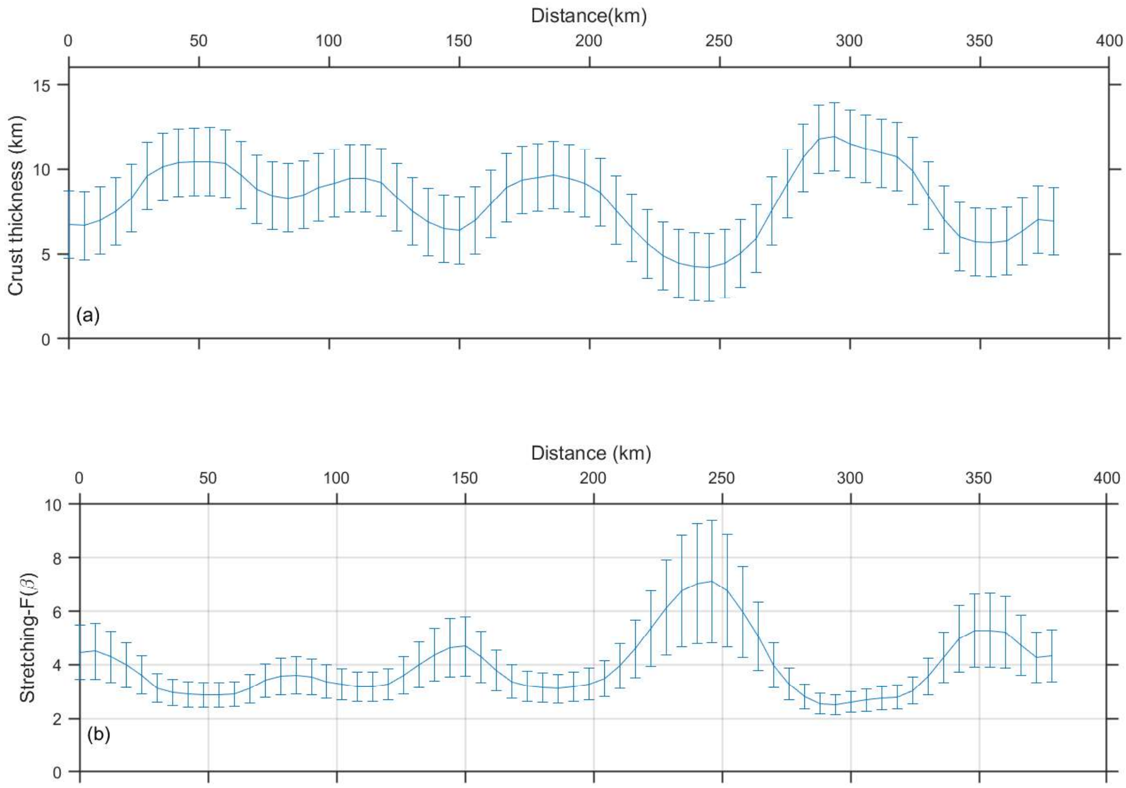

Figure 9. (a) Crustal thickness constrained by gravity modelling and PSTM seismic profile. Crustal thickness with ±2 km of uncertainty in picking of the basement from the PSTM seismic section and the Moho depth computation from gravity. (b) The stretching factor ($\beta=T_0/T_C$, T_0 is initial crust thickness and T_C is current crust thickness) of the corresponding profile.

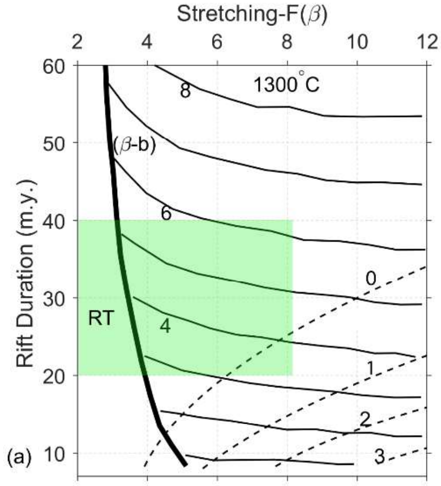

Figure 10. The varying rift duration with the effect of increasing amounts of extension β during rifting of the lithosphere with the potential temperature of 1300°C. The dashed lines show the thickness of melt produced (based on Bown & White 1995); black line is the stretching factor where the entire crust becomes brittle (based on Perez-Gussinye & Reston 2001); fine solid lines are the thickness of serpentinised mantle (on the basis of Perez-Gussinye & Reston 2001). Little to no volcanism is expected during the rifting for the Rockall Basin (green box shows the stretching factor and rift duration). However, the mantle serpentinisation is expected to be started at the observed stretching factor.

Supplementary material

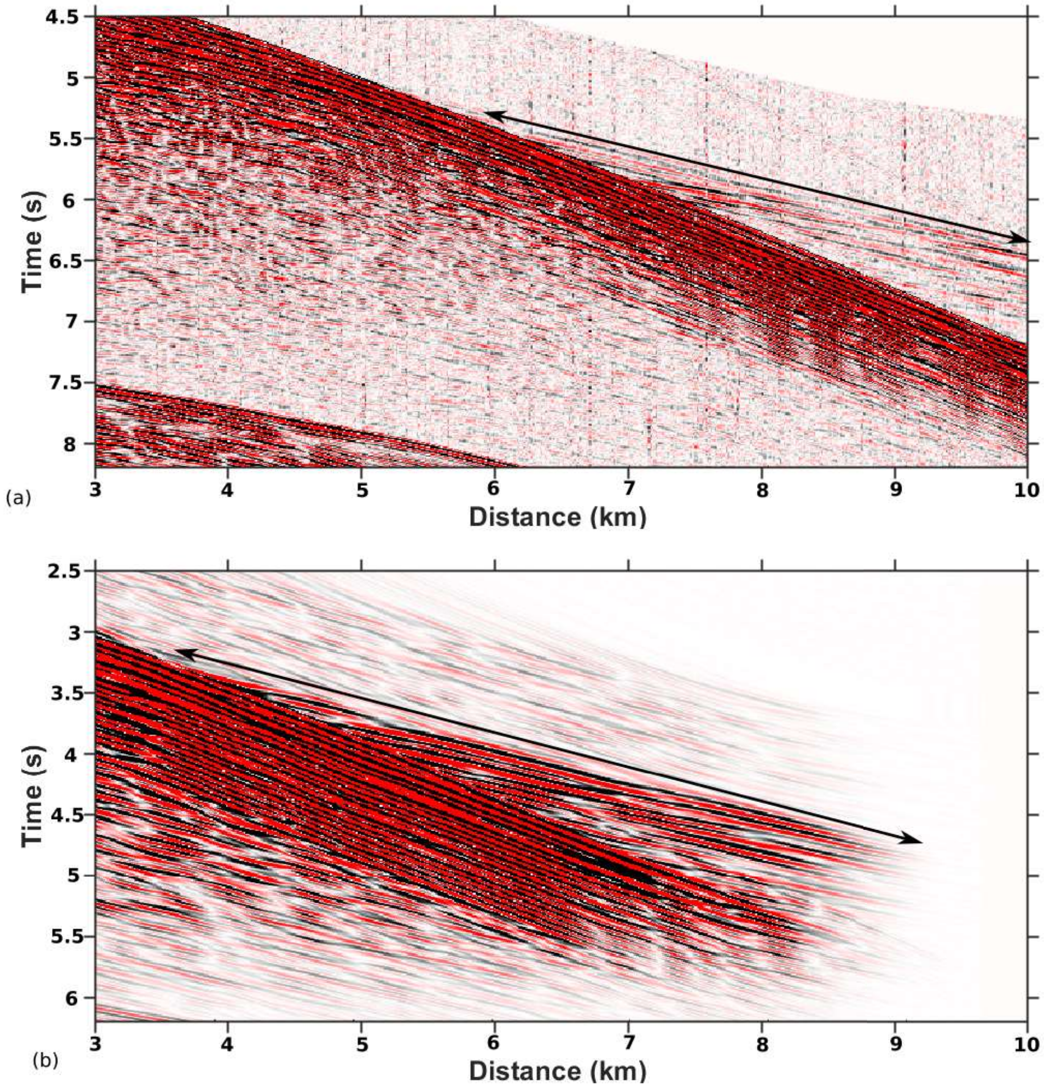

Figure S1 (a) Raw shot gather after pre-processing, (b) Downward continued shot gather. It can be seen that the first arrival is enhanced after downward continuation in comparison to the raw shot gather (with black arrow).

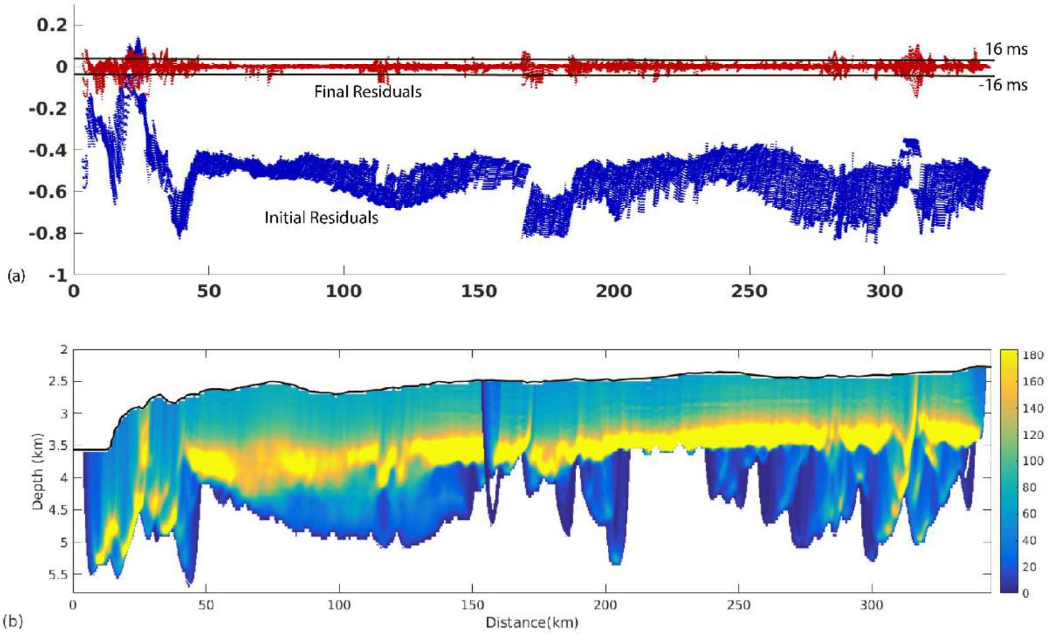

Figure S2. (a) initial (blue) and final residuals after the 14th iterations (red). After the 14th iteration χ^2 reaches 1.2. The residuals for this model are mainly within 16 ms (solid black lines), which is remarkably close to the uncertainty of 15 ms in the data (b) Derivative weighted sum (dws) of this model is masked, where ray coverage is < 8. The cyan line in Figure 5b is interpreted based on this dws value (<8).

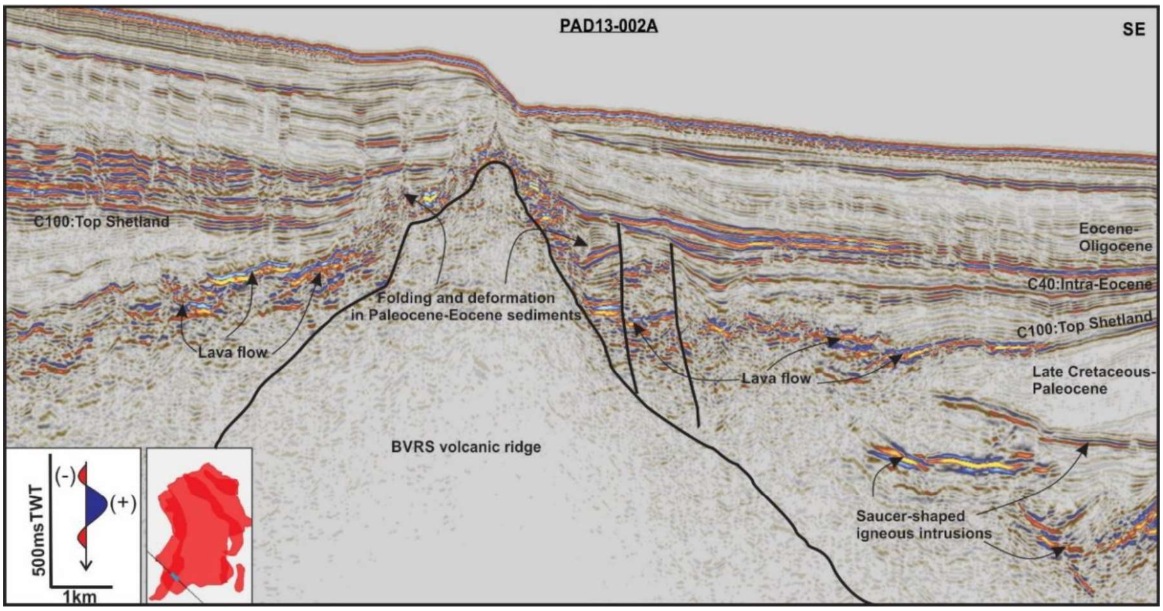

Figure S3. Interpretation of the BVRS at the profile from another location (shown in inset), this ridge is continuation of VR2 (Figure 4). The lava flow is observed at the boundary C100 (Shetland) similar to the VR1 (Figure 7c), which indicate that the BVRS was active during this period.

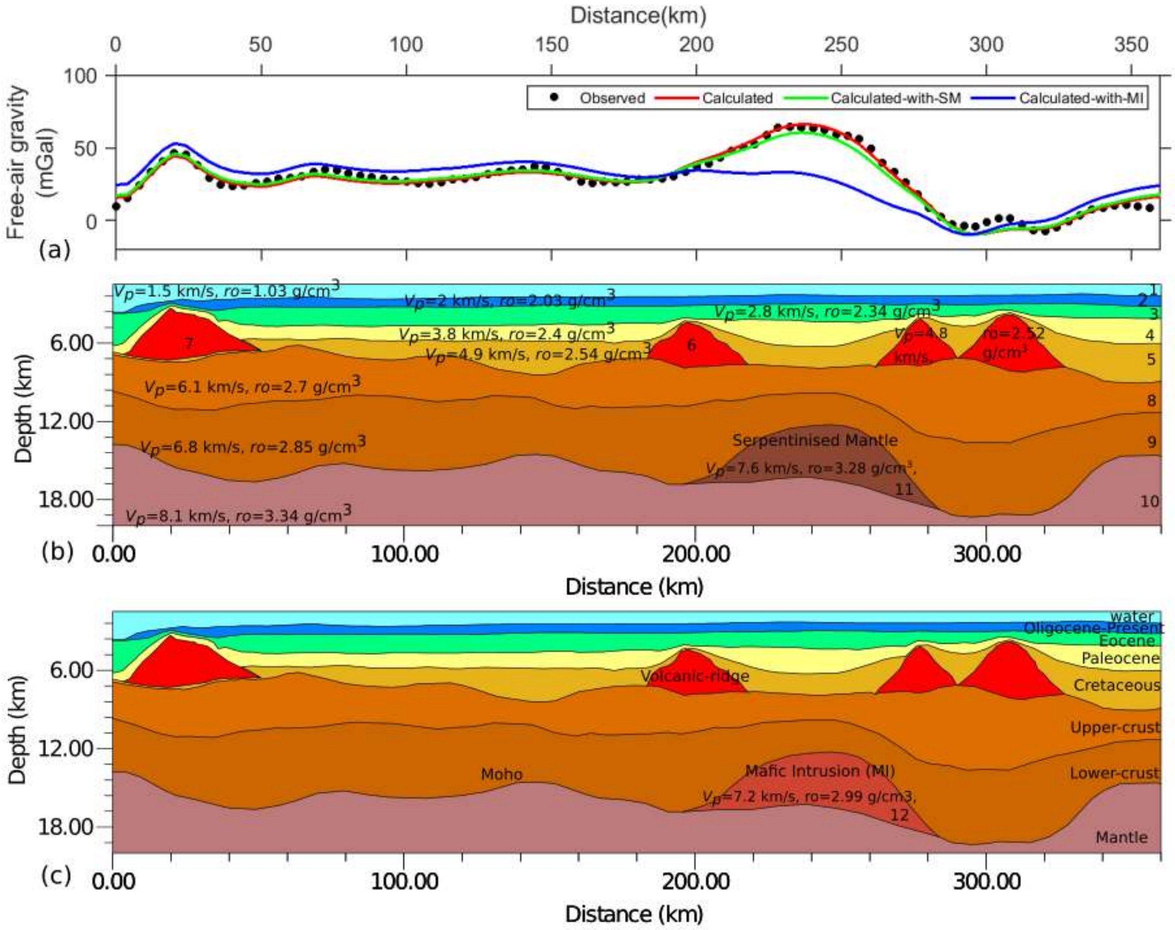

Figure S4 (a) Observed (black dots) and calculated gravity anomalies, red represent the calculated gravity anomaly using the geological model shown in Figure 6. Green and blue represent the calculated gravity anomaly using the geological model shown in (b) and (c) respectively. The model does not change if we consider the serpentinised mantle beneath the BVRS (b). The parameters (velocity, density, and magnetic susceptibility) used in the gravity modelling, are shown in Table 1. When considering mafic intrusion within the lower crust (c) this model does not fit the gravity anomaly.